# Airborne-laser-scanning-derived auxiliary information discriminating between broadleaf and conifer trees improves the accuracy of models for predicting timber volume in mixed and heterogeneously structured forests

Leo Gallus Bont [a,*], Andreas Hill [b], Lars T. Waser [c], Anton Bürgi [a], Christian Ginzler [c], Clemens Blattert [d]

*Corresponding Author

[a] Sustainable Forestry Group, Swiss Federal Institute for Forest, Snow and Landscape Research (WSL), Zuercherstrasse 111, CH 8903 Birmensdorf, Switzerland,

[b] Forest Service Rhineland-Palatinate, Beethovenstrasse 3, 54516 Wittlich, Germany

[c] Department of Land Change Science, Swiss Federal Institute for Forest, Snow and Landscape Research (WSL), CH 8903 Birmensdorf, Switzerland

[d] Department of Biological and Environmental Science, University of Jyväskylä, P.O. Box 35, 40014 Jyväskylä, Finland

**Highlights:**

- Information on forest type proportions improved the accuracy of volume predictions
- Forest type proportions weighted by canopy height outperformed area proportions
- The best model performance was obtained using forest type maps from leaf-off LiDAR

This document is the accepted manuscript version of the following article:
Bont, L. G., Hill, A., Waser, L. T., Bürgi, A., Ginzler, C., & Blattert, C. (2020). Airborne-laser-scanning-derived auxiliary information discriminating between broadleaf and conifer trees improves the accuracy of models for predicting timber volume in mixed and heterogeneously structured forests. Forest Ecology and Management, 459, 117856 (18 pp.). https://doi.org/10.1016/j.foreco.2019.117856

# Abstract

Managing forests for ecosystem services and biodiversity requires accurate and spatially explicit forest inventory data. A major objective of forest management inventories is to estimate the standing timber volume for certain forest areas. In order to improve the efficiency of an inventory, field based sample-plots can be statistically combined with remote sensing data. Such models usually incorporate auxiliary variables derived from canopy height models. The inclusion of forest type variables, which quantify broadleaf and conifer volume proportions, has been shown to further improve model performance. Currently, the most common way of quantifying broadleaf and conifer forest types is by calculating the proportions of the corresponding areas of the canopy cover. This practice works well for single-layer forests with only a few species, but we hypothesized that this is not best practice for heterogeneously structured and mixed forests, where the area proportion does not accurately reflect the timber volume proportion. To better represent the broadleaf and conifer volume proportions, we introduced two new auxiliary variables in which the area proportion is weighted by height information from a canopy height model.

The main objectives of this study were: (1) to demonstrate the advantage of including forest type (broadleaf/conifer distinction) information in ordinary least squares regression models for timber volume prediction using widely available data sources, and (2) to investigate the hypothesis that including the broadleaf and conifer proportions, weighted by canopy height information, as additional auxiliary variables is favourable over including simple area proportions. The study was conducted in three areas in Switzerland, all of which have heterogeneously structured and mixed forests. Our main findings were that the best model performance can generally be achieved: (1) by deriving conifer and broadleaf proportions from a high-resolution broadleaf/conifer map derived from leaf-off airborne laser scanning

data, and (2) by using broadleaf/conifer proportions weighted by height information from a canopy height model. Incorporating the so-derived conifer and broadleaf proportions increased the model accuracy by up to 9 percentage points in root mean square error (RMSE) compared with models not using any forest type information, and by up to 2 percentage points in RMSE compared with models using conifer and broadleaf proportions based solely on the corresponding area proportions, as done in current practice. Our findings are particularly relevant for mixed and heterogeneously structured forests, such as those managed to achieve multiple functions or to adapt effectively to climate change.

**Keywords:** airborne laser scanning, best fit models, canopy height model, forest type map, high-precision forest inventory, image-based point clouds, mixed and heterogeneously structured forest, ordinary least squares regression models, merchantable timber volume

# 1 Introduction

Forest ecosystems provide multiple benefits for humans and are particularly important for the conservation of biodiversity (Bäck et al., 2017; MEA, 2005). These manifold contributions of forests make their management a complex and challenging task requiring accurate and spatially explicit information. The aim of forest inventories in general is to obtain reliable information on the condition and development of the forest (Barrett et al., 2016). As the census of an entire forest area is usually impossible, because of the high costs involved, sampling concepts are used in practice. With these methods, the local hectare density of timber volume, basal area and many other forest attributes are derived from measurements of the trees in randomly or systematically distributed sample-plots in the forest area. This data is then used to estimate mean values and totals for the entire forest area, for example the mean or the total timber stock.

More accurate information on an entire forested area or a small area (e.g. parts of a forest enterprise) can be obtained by complementing field based inventories with remote sensing data. Furthermore, this can be a cost-effective alternative to increasing the number of field based sample units. The principle of such two-phase inventories is to use statistical models to predict response variables, such as basal area or timber volume, for the population units where no field data is available. Many studies have already demonstrated the potential of these methods (e.g. Hill et al., 2018; Magnussen et al., 2014; Mandallaz et al., 2013; Næsset, 2004, 2002; Steinmann et al., 2013). Usually, such statistical models are based on auxiliary variables derived from a canopy height model (CHM) (Xu et al., 2019). Other sources of information, such as tree species or forest type (we use the term ‘forest type’ for the distinction between either conifer and broadleaf trees or evergreen and deciduous trees,

see section 2.2) have been added in a few case studies to improve the performance of the models (Gabriel et al., 2018; Hill et al., 2018).

For Switzerland, a freely available national forest type map (FTM) based on optical remote sensing data (Waser et al., 2017) exists in the framework of the Swiss National Forest Inventory (NFI). FTMs can also be derived using multi-temporal (i.e. leaf-on, leaf-off) laser scanning data. Such an approach entails collecting two Light Detecting and Ranging (LiDAR) datasets at the same site under leaf-off and leaf-on conditions (Liang et al., 2007). Alternatively, forest types can be derived based on return intensity and ranking distributions of laser scans from a single point in time, preferably under leaf-off conditions for the conifer/broadleaf differentiation (Liang et al., 2007; Ørka et al., 2009; Parkan, 2018). However, deciduous conifers (i.e. conifers which defoliate in autumn, such as larch) cannot be identified as conifers with any of these three approaches (Fassnacht et al., 2016).

FTM information has been used in many studies to improve standing timber volume estimations. For example, Breidenbach et al. (2008) used a continuous variable 'conifer proportion' and its interaction term with the average canopy height to include FTM information derived from leaf-off LiDAR data. Latifi et al. (2012) formed a FTM based on colour infrared (CIR) orthoimages and included the forest type as a categorical variable in their model. The forest type of the sample-plots was assigned to either broadleaf or conifer if the proportion of the pixels of one particular type exceeded 70%, and it was assigned to the mixed category in all other cases. Straub et al. (2009) used CIR orthoimages to create a FTM. They derived the conifer and broadleaf proportions from the percentages of the corresponding pixels in each sample-plot, and this information was then included in the model to estimate the stem volume of forest stands. Hill et al. (2018) included information on five tree species as a categorical variable to improve timber volume predictions. Finally, in

105 Nordic countries such as in Finland, including tree species information as auxiliary data to
106 predict timber volume is quite common, as described by Kukkonen et al.( 2019, 2018),
107 Packalén and Maltamo (2006) and Räty et al. (2016).

108 All of the approaches mentioned above have led to a significant improvement in the
109 accuracy of standing timber volume predictions by including forest type or tree species
110 information in the models. However, in all these studies forest type proportion information
111 was derived based on the area covered by the canopy of the corresponding forest type. This
112 current practice works well for even-aged and single-layer forests. However, we hypothesize
113 that this approach is not best practice for heterogeneously structured and mixed forests, in
114 which different age classes and tree species can occur across a small surface (e.g. within a
115 sample-plot). In such forests the area proportion does not adequately reflect the timber
116 volume proportion. There are two possible reasons for this discrepancy. First, the mean tree
117 size might differ depending on the canopy height. To illustrate this possibility we consider a
118 sample-plot on which conifer and broadleaf trees cover about the same amount of area and
119 where the conifers are all mature whereas the broadleaf trees are much younger. In this
120 case the volume on the half of the sample-plot with the young broadleaf trees is clearly
121 smaller than that on the half with the mature coniferous trees. This point has been
122 confirmed in studies about allometric relationships, such as the work by Reineke, (1933) in
123 establishing the self-thinning rule. In this case, using the area proportion of conifers leads to
124 an underestimation of the proportion of conifer timber volume. Second, stand density (the
125 number of stems in a certain area) also differs for the different species. This point was
126 shown by Pretzsch and Biber (2005) and by Rivoire and Le Moguedec (2012), who
127 generalized the self-thinning relationship of Reineke (1933) for multi-species and mixed-size
128 forests.

129 To better represent the volume proportion of different forest types, in this study we
130 introduced two new forest type variables (FTVs), referred to as 'weighted-canopy-height
131 proportions', in which the area proportions are weighted by height information from a
132 canopy height model. We hypothesized that the 'weighted-canopy-height-proportion' FTVs
133 are favourable over simple area proportion FTVs in mixed and heterogeneously structured
134 forests.

135 The overall objectives of the present study were: (1) to determine the advantage of including
136 forest type information in regression models for timber volume prediction using existing and
137 forthcoming data sources, and (2) to investigate the hypothesis that the 'weighted-canopy-
138 height proportion' FTVs are favourable over simple area proportion FTVs. Both aims are of
139 high practical interest because the underlying data sources used to derive the FTVs, such as
140 the national broadleaf/conifer map or the national leaf-off airborne laser scanning (ALS)
141 data, are widely available and can be integrated with a small effort into current inventories.
142 However, neither of these sources have been used operationally for inventory purposes. This
143 work was embedded in the implementation of design-based regression estimators
144 (Mandallaz, 2013) for predicting standing timber volume. As these design-based regression
145 estimators rely on ordinary least squares (OLS) regression, we used OLS regression models in
146 our study.

147 We addressed the following specific research questions:

148 (1) Is there a gain in model performance when the new 'weighted-canopy-height proportion'
149 FTVs are incorporated into OLS regression models for predicting timber volume, compared
150 with models including the simple area proportion FTVs and models with no forest type
151 explanatory variables?

(2) Is there a common best practice for integrating FTM information, such as the spatial resolution considered, that is independent of the individual LiDAR and FTM characteristics?

# 2 Materials and Methods

## 2.1 Study areas

We studied the effect of incorporating different FTV alternatives in three independent study areas in Switzerland: Bremgarten (Brg), Glâne-Farzin (GF) and Sarine (SA) (Figure 1). All three study areas are heterogeneously structured and mixed temperate forests of conifer and broadleaf species, but they have different properties in terms of age-class structure.

### 2.1.1 Bremgarten (Brg)

In Brg, the latest forest inventory data from 2011/2012 was used as input. This data is based on permanent sample-plots on an 80 m x 150 m grid, as described by Schmid-Haas (2003). The location of the sample-plots is shown in Figure 1. A total of 363 sample-plots were measured, with an average timber volume of 274 $m^3$ $ha^{-1}$, 55% of which is conifer wood (Table 1). The distribution of the timber volumes of the sample-plots indicates that stands with large timber volumes are under-represented compared with a normal age-class structure (Salo and Tahvonen, 2002) (Figure 2). This unbalanced age-class structure of the forest was caused by the storm Lothar in December 1999, which primarily damaged mature stands. Figure 3 shows that sample-plots with a large timber volume are dominated by the conifer volume, whereas sample-plots with a small volume are dominated by the broadleaf volume. LiDAR data was acquired in November 2011, providing excellent temporal synchronization between the field based and the remote sensing data. The density of the LiDAR raw data is at least 8 points $m^{-2}$ and is comparable with values in the other study areas (Table 1).

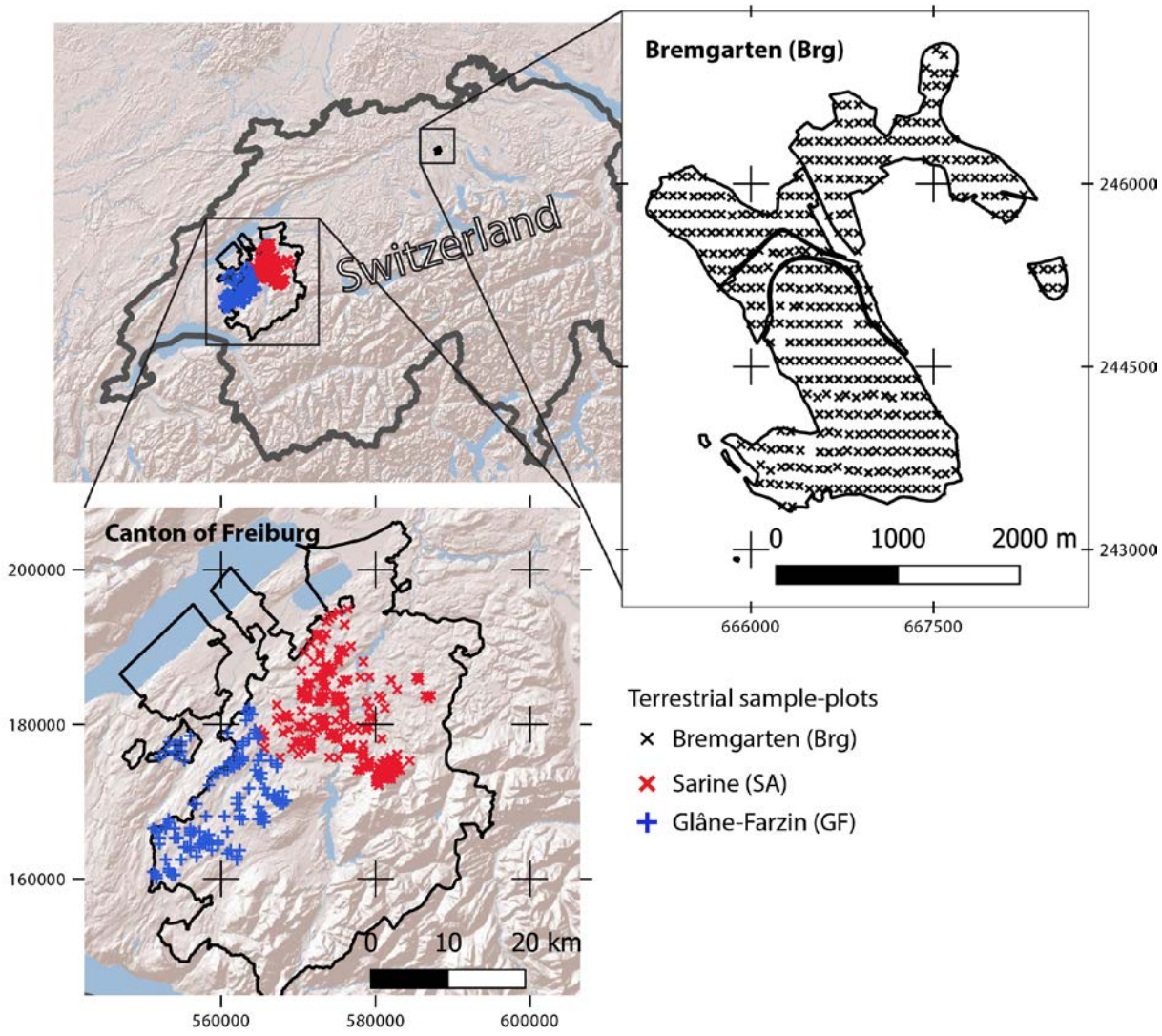


**Figure 1: Investigated case study areas in Switzerland and the distribution of the permanent sample-plots (coordinate system: EPSG 21781, CH 1903 / LV 03 ).**

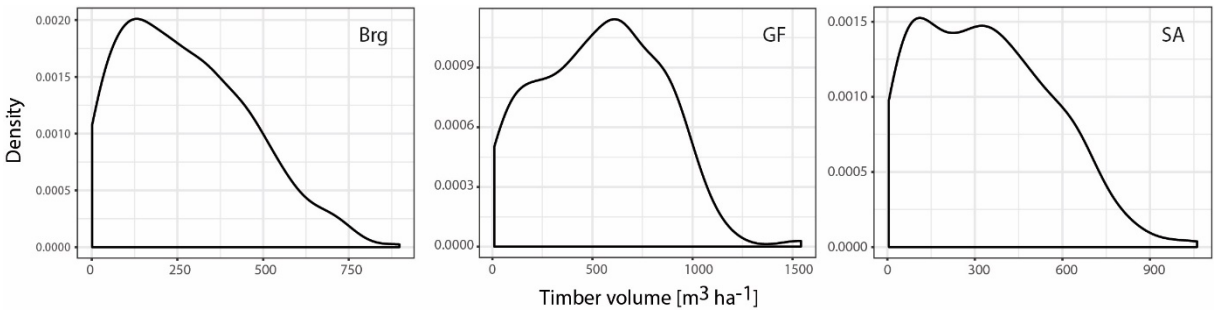


**Figure 2: Local densities of the measured timber volume distributions on the field based sample-plots for Bremgarten (Brg), Glâne-Farzin (GF) and Sarine (SA). The scales for both axes differ among panels.**

| | Bremgarten (Brg) | Glâne-Farzin (GF) | Sarine (SA) |
|---|---|---|---|
| Number of field based sample-plots | 363 | 137 | 202 |
| Number of sample-plots after cleaning (see section 2.6) | 341 | 131 | 194 |
| Number of sample-plots after cleaning and removing sample-plots containing larch | 304 | 125 | 184 |
| Theoretical grid size of sample-plots | 80 m x 150 m | 400 m x 400 m | 400 m x 400 m |
| Exact measurement of the sample-plot centres | Yes, DGPS measurement with precision of 1 m available | No, only theoretical position known | |
| Recording method | 400 $m^2$ circle, min DBH threshold for recording: 12 cm (Schmid-Haas et al., 1993) | 3 concentric circles:<br>[I] 200 $m^2$ circle with DBH threshold of 12 cm<br>[II] 300 $m^2$ circle with DBH threshold of 16 cm<br>[III] 500 $m^2$ circle with DBH threshold of 36 cm (Keller, 2013) | |
| Date of measurements on the sample-plots | Autumn – Winter 2011/2012 | Autumn 2016 | Autumn 2017 |
| Date of the LiDAR flight | 9.11.2011 | 07.10.2016 until 12.02.2017, mostly leaf-off condition but leaf-on also partially available | |
| Point density of the LiDAR raw data | ≥ 8 points $m^{-2}$ | ≥ 5 points $m^{-2}$ | ≥ 5 points $m^{-2}$ |
| GPS receiver and precision | DGPS receiver, 1 m precision | SXBlue II+ GNSS, 2.5 m horizontal precision | SXBlue II+ GNSS, 2.5 m horizontal precision |

**Table 1: Properties of the study areas Bremgarten, Glâne-Farzin and Sarine (DBH = diameter at breast height, 1.3 m above the ground).**

### 2.1.2 Glâne-Farzin (GF)

In GF, the inventory data from 2016 was used as input, which is based on 137 permanent sample-plots on a 400 m x 400 m grid (Figure 1). With a horizontal accuracy of 2.5 m, the sample-plot centres are less accurate than in Brg, as georeferencing with a differential GPS (DGPS) was not available. However, this precision was provided by the manufacturer of the GPS receiver, which might be too optimistic under a forest cover (Lamprecht et al., 2017). Even with DGPS an accuracy of 2.5 m is not feasible (Lamprecht et al., 2017). Further characteristics and properties of the study area are listed in Table 1. Compared with Brg, the forests in GF are more homogeneous and mainly dominated by conifers. The mean timber volume is 534 $m^3$ $ha^{-1}$, 70% of which is conifer wood. Sample-plots with a large timber

volume are overrepresented compared with a normal age-class structure (Figure 2), and, according to the volume ratio, conifers dominate these sample-plots (Figure 3). The LiDAR flight was carried out between November 2016 and February 2017, and it again provided excellent temporal synchronization between terrestrial and remote sensing data. In the majority of cases, data was collected under leaf-off conditions. The density of the LiDAR raw data is at least 5 points $m^{-2}$.

### 2.1.3 Sarine (SA)

The inventory in SA consists of 202 sample-plots and was last conducted in 2017. SA is, like GF, located in the canton of Freiburg and thus has the same inventory design (Table 1). The average timber volume of the sample-plots is 335 $m^3$ $ha^{-1}$, 55% of which is conifer wood. Inventory sample-plots indicate that stands with a small timber volume are slightly overrepresented compared with a normal forest age-class structure (Figure 2). Overall, however, forests in this study area are well balanced in terms of age-class structure. Compared with GF, where most sample-plots are conifer dominated, most sample-plots in SA are mixtures of conifer and broadleaf trees (Figure 3). The LiDAR data originates from the same flight as used for GF and has the same characteristics.

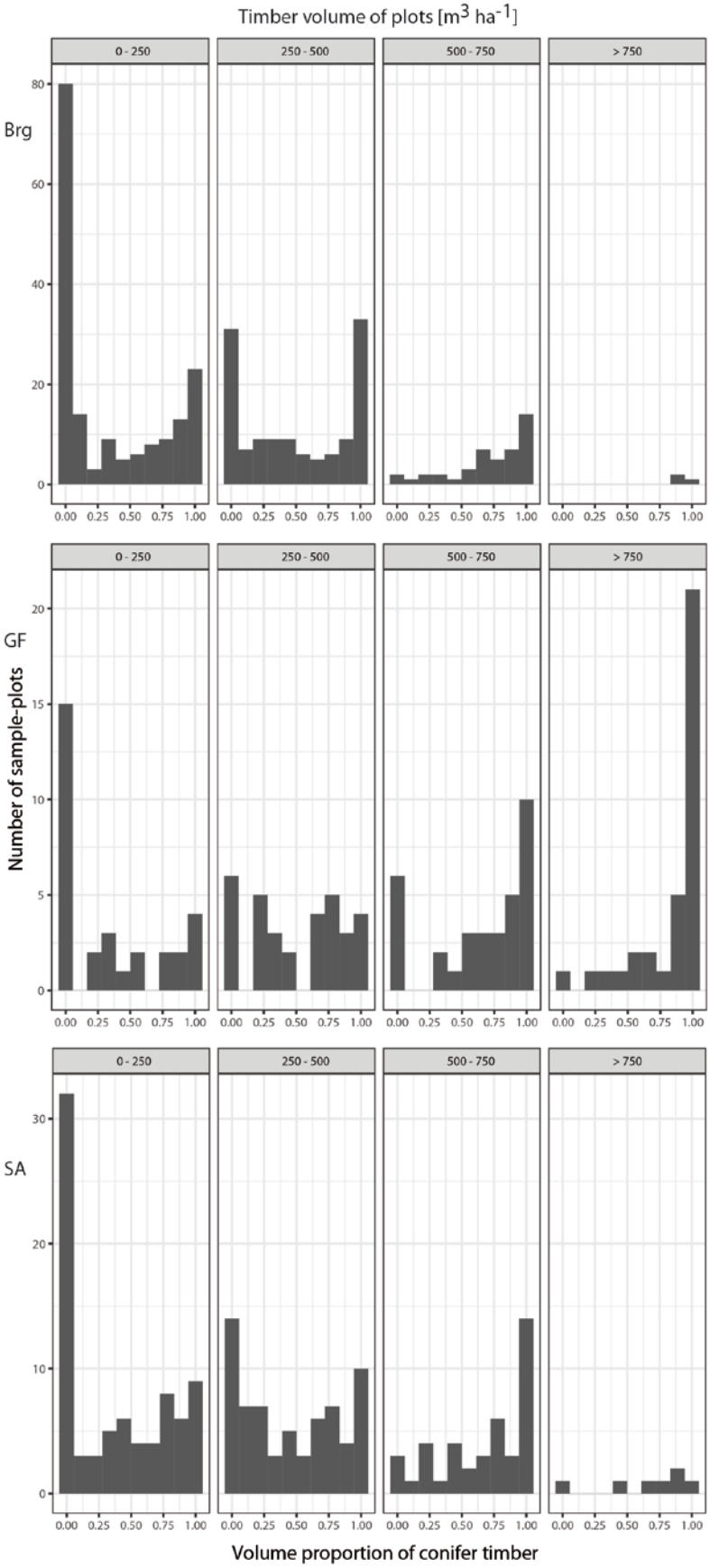


**Figure 3: Proportion of conifer timber volume on the terrestrial sample-plots in Bremgarten (Brg), Glâne-Farzin (GF) and Sarine (SA) for different timber volume densities (< 250, 250–500, 500–750 and > 750 $m^3$ $ha^{-1}$). The scale on the y-axis differs among panels.**

## 2.2 Forest type maps (FTM)

We used five types of FTMs. Table 2 gives an overview of them and Figure 4 shows the information they contain and their resolution for a detail in the study area Brg. As some FTMs distinguish between trees that are foliated throughout the year and trees that are only foliated during the vegetation period (evergreen/deciduous) whereas others distinguish between conifers and broadleaf trees, Table 2 additionally indicates the forest type differentiation of each map. This differentiation is particularly relevant if larch (*Larix decidua*, a deciduous conifer) is present. However, to have a proper experimental design that differentiates between broadleaf and conifer trees for all FTMs, sample-plots that include larch were removed, as explained in detail in section 2.6.

| Description | Resolution [m] | Acquisition of raw data [year] | Forest type distinction |
|---|---|---|---|
| Orthoimage (OI) | 2 m x 2 m | 2014 (only Brg available) | evergreen / deciduous |
| Swiss NFI Orthoimage (NFI) | 3 m x 3 m | 2010–2016 | conifer / broadleaf |
| Sentinel NFI (Sen) | 10 m x 10 m | 2016–2017 | conifer / broadleaf |
| Copernicus Dominant Leaf Type (DLT) | 20 m x 20 m | 2012 (Brg) / 2015 (GF, SA) | conifer / broadleaf |
| LiDAR (based on return intensity leaf-off) (LI) | 0.5 m x 0.5 m | 2014 (Brg) / 2016 (GF, SA) | evergreen / deciduous |

**Table 2: Overview of the forest type maps (FTMs) used in the study. Brg = Bremgarten, GF = Glâne-Farzin (GF) and SA = Sarine.**

### 2.2.1 Orthoimage (OI)

The FTM orthoimage (OI) is based on leaf-off (winter 2014) and leaf-on (summer 2014) digital aerial stereo imagery (Table 2). A digital surface model was calculated using the stereo-images from summer 2014. It was normalized with the digital terrain model 'swissAlti3D' to derive a canopy height model (CHM). This CHM was used to orthorectify the image datasets from both winter and summer 2014. For both orthoimages the normalized difference vegetation index (NDVI) was calculated. Thus, a winter dataset that represents evergreen vegetation taller than 3 m and a summer dataset that represents both evergreen

235 and broadleaf vegetation taller than 3 m were produced. The two datasets were combined
236 to retrieve the FTM. Therefore, this FTM distinguishes between evergreen and deciduous
237 trees (Figure 4a).

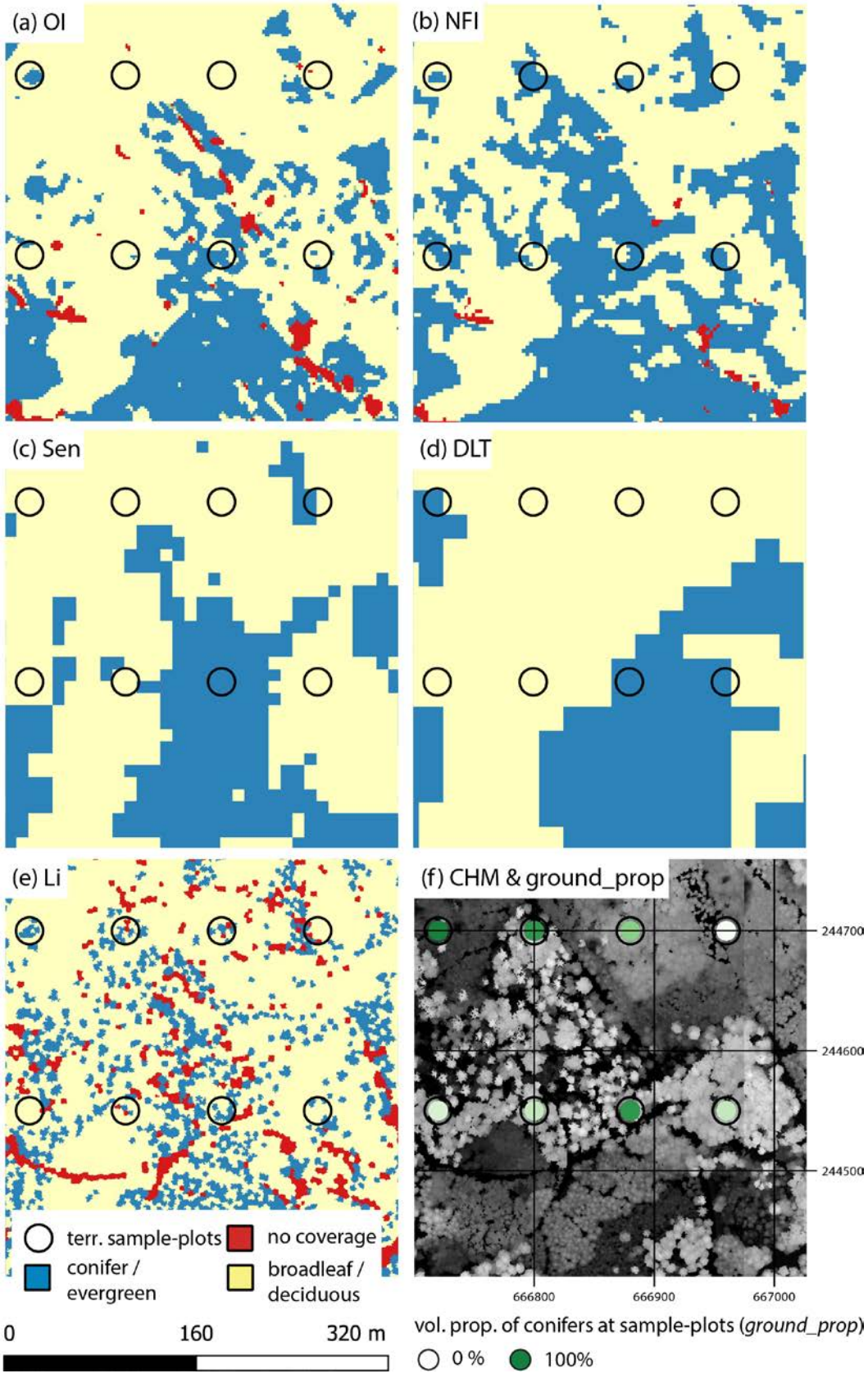


**Figure 4: (a) – (e) Forest type maps (FTMs) and (f) canopy height model (CHM) for a sub-area around eight field based inventory sample-plots in the study area Bremgarten (coordinate system: EPSG 21781, CH 1903 / LV 03) (Li = LiDAR, Sen = Sentinel NFI, NFI = Swiss NFI Orthoimage, OI = Orthoimage, DLT = Copernicus Dominant Leaf Type). For (a) and (e) the FTM differentiates between evergreen and deciduous foliage; for (b), (c) and (d) the FTM differentiates between conifer and broadleaf trees.**

### 2.2.2 Swiss NFI Orthoimage (NFI)

This map distinguishes between broadleaf and conifer trees (Waser et al., 2017) and was produced for the Swiss National Forest Inventory (NFI). It covers all of Switzerland and has a spatial resolution of 3 m x 3 m. The methodology is based on the classification of more than 1700 four-band aerial photo strips. Prior to applying it to all of Switzerland, different classification methods, i.e. Support Vector Machine, Logistic Regression and Random Forest (RF) were tested for selected areas in Switzerland regarding accuracy, computing time and minimum number of required training values. The tests revealed that RF performed best regarding accuracy and processing time (Waser et al., 2017; Figure 4b).

### 2.2.3 Sentinel NFI (Sen)

The FTM sentinel NFI is a national FTM that distinguishes between broadleaf and conifer trees at a spatial resolution of 10 m.

This map is based on freely available spaceborne Sentinel-1 / -2 data from the European Space Agency's Copernicus Programme (ESA, 2019). In order to get a cloud-free coverage of all of Switzerland, a total of 50 Sentinel-2 images from June, July and August of 2016–2018 were used. The Sentinel-1 SAR data was acquired in summer 2016 and 2017 and processed, i.e. flattening terrain and increasing the spatial resolution, according to Small (2012). This map is a product of the Swiss NFI, and it is a follow-up and improved version of the preliminary dataset (referred to as FTM NFI) and is free from overestimations of conifers caused by topographic and illumination effects. This new approach incorporates a RF classifier. According to Breiman (2001), this is a widely used ensemble classifier that produces multiple decision trees using a randomly selected subset of training samples and variables (Figure 4c).

### 2.2.4 Copernicus Dominant Leaf Type (DLT)

The FTM Dominant Leaf Type (DLT) is a product of the Copernicus Land Monitoring Service coordinated by the European Environment Agency. The DLT FTM provides information on the dominant leaf type (broadleaf or conifer) at a 20 m x 20 m resolution, and it was derived from multi-temporal satellite image data using Support Vector Machine (Langanke, 2017; Figure 4d).

### 2.2.5 LiDAR (Li)

The FTM LiDAR differentiates between deciduous and evergreen foliage and was computed by using the corrected return intensity of leaf-off airborne laser scanning (ALS) data, as proposed in the Digital Forestry Toolbox (Parkan, 2018). The FTM LiDAR has a spatial resolution of 0.5 m and was computed for GF and SA from the same leaf-off data as used for the CHM and for Brg from a leaf-off flight from March 2014 with a density of > 10 points $m^{-2}$. This map has great potential for application because leaf-off ALS data is widely available and calculation with the Digital Forestry Toolbox is straightforward (Figure 4e).

## 2.3 Canopy height model (CHM)

We used the LiDAR raw point data (Table 1) to compute pit-free CHMs. This approach for CHM calculation avoids gaps ('pits'), following the methods presented by Isenburg (2014) and Khosravipour et al. (2014). This algorithm was implemented in LAStools (Rapidlasso GmbH, Gilching, Germany), but also using the package 'lidR' (Roussel and Auty 2017) in R version 3.5 (R Core Team, 2018). An example of a pit-free CHM is given in Figure 4. The CHMs produced in this study have a spatial resolution of 0.33 m (Figure 4f).

## 2.4 Response variable

The response variable is the local density of the merchantable timber volume [$m^3$ $ha^{-1}$] (volume of the stem and branches with a diameter ≥ 7 cm) and is referred to as *VOL* in the model formulation. The field measurements were carried out according to the sampling

protocol of Keller (2013) for GF and SA and of Schmid-Haas et al. (1993) for Brg. In all study sites, only the DBH (diameter at breast height, measured at 130 cm above the level of the terrain) was recorded. For the calculation of the timber volume of a single tree (*VOL_ST*) in Brg, the following one-parameter volume function of Hoffmann (1982) was used: $VOL\_ST(DBH) = exp\left(a_1 + a_2 ln(DBH) + a_3\left(ln(DBH)\right)^4\right)$, with the parameters $a_1$, $a_2$ and $a_3$ and with *DBH* as the only input variable. In GF and SA a volume function based on volume tables was used (Schweizer, 2012), again with DBH as the only input variable. This volume function was chosen to ensure comparability with earlier inventories. While in SA and GF the same volume function was used for trees of both leaf types, in Brg separate volume functions were used for broadleaf and coniferous trees. However, a comparison of the functions showed that the differences in the predicted tree volumes between the volume functions differentiating by forest type (Brg) and the mixed volume functions (GF and SA) were marginal (Figure 5). Clear differences only emerged at ≥ 100 cm DBH. However, this has no relevance for the present study, as only four sample trees were above this DBH threshold. As volume functions are not valid for large areas, they have to be calibrated locally. The parametrization of the volume function in Brg was done during the inventory of 1986. For this purpose, the height (h), DBH and diameter at 7 m height ($d_7$) was measured for all sample trees in one-eighth of each sample-plot area (for trees with a DBH < 20 cm), in one-quarter of each sample-plot area (20 cm ≤ DBH < 50 cm) or in the entire sample-plot (DBH ≥ 50 cm) (Schmid-Haas et al., 1993). With the help of three-parameter volume functions requiring h, DBH and $d_7$ as input, a reference volume was then calculated for all sample trees that were measured in detail. Finally, a nonlinear curve fitting method was used to determine the locally adapted parameters $a_1$, $a_2$ and $a_3$ (Hoffmann, 1982).

To ensure comparability with previous inventories, we therefore used the parameters derived in 1986. A validation of the volume functions used in Brg was done by Kaufmann (2001). He reported a coefficient of determination ($R^2$) of 95% and a standard deviation of the residuals ($R_s$) of 20% (conifer) and 27% (broadleaf) of the mean. The local density of the total timber volume on each terrestrial sample-plot was based on the timber volume and inclusion probabilities of individual trees and was calculated using the Horvitz Thompson Estimator (Mandallaz, 2007).

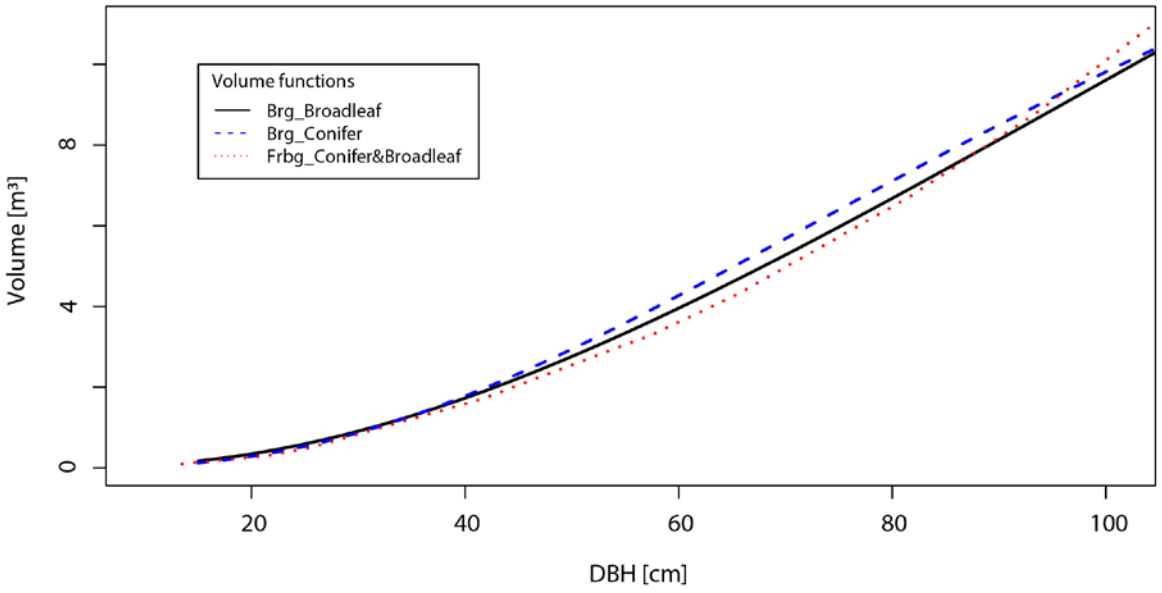


**Figure 5: Volume functions for Glâne-Farzin and Sarine in canton Freiburg (Frbg) and for Bremgarten (Brg).**

## 2.5 Auxiliary variables

### 2.5.1 Auxiliary variables based on canopy height models

Auxiliary variables form the basis for model building and were used to derive a model for the response variable (*VOL*) from the sample data. Auxiliary variables can come from various sources, such as LiDAR raw data, CHMs and FTMs. An overview of auxiliary variables that are potentially interesting for forestry can be found in McCallum et al. (2014) and Saarela et al. (2015). Auxiliaries derived from the CHM, which were used in our models, are listed in Table 3.

Most of the auxiliary variables included in this study are well established for forest inventory purposes. However, to the best of our knowledge, the variable *SSq* has not previously been described in the literature. It is presented in detail in Figure 6a and represents the sum of the squares of the height values of the individual CHM-pixels within a sample-plot. The idea behind introducing this auxiliary variable was to make it possible to map the allometric relationships more appropriately, as the stand volume is usually not a linear function of the canopy height (Eichhorn, 2013; Pretzsch, 2001).

| | **Description** | **Abbreviation** | **Unit** |
|---|---|---|---|
| Percentile – values | Specifies the height percentiles of the pixels in the sample-plot. Example: 95th percentile: P95 | PXX<br>XX = {99, 95, 90, 80, 75, 70, 60, … , 30, 25, 20, 10, 05, 01} | [m] (same unit as the CHM) |
| Coverage – values | Indicates the vegetation cover at a certain height. Example: 2 m coverage: C02 = 0.9 means that 90% of the pixels of the vegetation height model in the plot are higher than or equal to 2 m above the ground. | CXX<br>XX = {00, 02, 05, 10, 15, 20, … , 50} | [0 – 1] |
| Minimum | Minimum pixel value within a plot | MIN | [m] |
| Maximum | Maximum pixel value within a plot | MAX | [m] |
| Standard deviation | Standard deviation of the individual pixels within a plot | STD | [m] |
| Average | Average value (height) of the individual pixels within a plot | MEAN | [m] |
| Sum of squares | Sum of the squares of the individual pixels within a plot | SSq | |
| Average sum of squares | Sum of squares divided by number of pixels in a plot | MSSq | |
| Coefficient of variation | MEAN / STD | CV | |

**Table 3: Auxiliary variables derived from the canopy height model (CHM).**

(a)

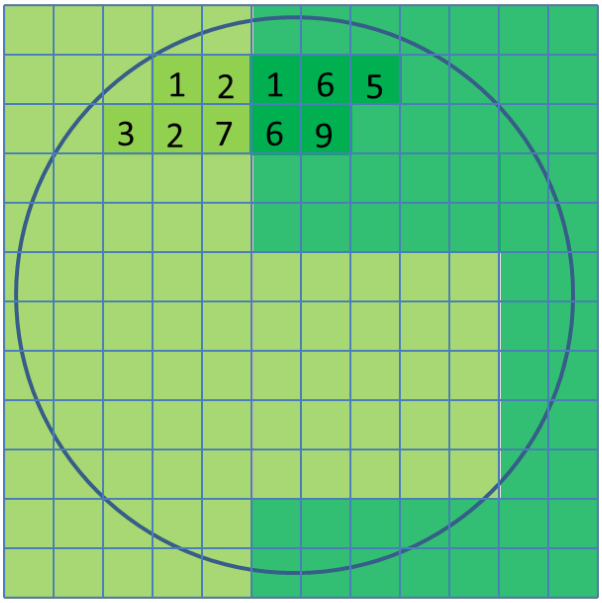


$SSq = 1^2 + 2^2 + 1^2 + 6^2 + 5^2 + 3^2 + 2^2 + 7^2 + 6^2 + 9^2 = 246$

$SSq\_Broadleaf = 1^2 + 6^2 + 5^2 + 6^2 + 9^2 = 179$

$SSq\_Conifer = 1^2 + 2^2 + 3^2 + 2^2 + 7^2 = 67$

2 Canopy height [m] (source: CHM)

Broadleaf pixel (source: FTM)

Conifer pixel (source: FTM)

(b)

| | ① number of pixels | ② sum of canopy height | ③ SSq of canopy height |
|---|---|---|---|
| conifer | 5 | 15 | 67 |
| broadleaf | 5 | 27 | 179 |
| total | 10 | 42 | 246 |
| ⇩ | area_prop | area_chm_prop | area_chm_sq_prop |
| proportion of conifer | 0.50 | 0.36 | 0.27 |

**Figure 6: Principle of the combined evaluation of different grids. The two grids forest type map (FTM) (conifer/broadleaf) and canopy height model (CHM) are superimposed and evaluated for each attribute of the FTM. a) Illustration of the derivation of the auxiliary variable SSq (sum of squares), based on a combined evaluation of the CHM and the FTM. The circle represents the boundary of the sample-plot. b) Computation of the different forest type variable alternatives: 1) ratio of the number of pixels (area_prop), 2) ratio of the sums of canopy height (area_chm_prop), and 3) ratio of the sums of squares of the canopy heights (area_chm_sq_prop). Most pixels in (a) are empty to simplify the comprehensibility of the calculations. If the FTM and the CHM have different spatial resolutions, the analysis is performed on the basis of the grid with a higher spatial resolution.**

### 2.5.2 Forest type variables (FTV)

In order to include FTM information in the statistical models, auxiliaries (referred to as forest type variables, FTV) were introduced that describe the proportion of conifer trees. There were five FTV alternatives: four continuous and one categorical. The continuous FTV alternatives were: (1) the ratio of the number of pixels of different forest types (*area_prop*), (2) the ratio of average heights of the forest types (*area_chm_prop*), (3) the ratio of the sum of squares of the canopy heights of the forest types (*area_chm_sq_prop*) (see Figure 6b),

and (4) the variable *ground_proportion*, which is introduced in section 2.5.3. *area_prop* is the classical formulation and represents the proportion of the area that is covered by the canopies of conifers. *area_chm_prop* and *area_chm_sq_prop* were our new 'weighted-canopy-height proportion' FTVs, for which the area proportion was weighted by information from a CHM. Therefore, the two grids (CHM and FTM) were superimposed and a separate evaluation was performed for each forest type, as presented in Figure 6a and b. For the categorical variable, we chose a setup that assigns the sample-plot to a main forest type (broadleaf or conifer) if the proportion of the pixels of one particular type exceeds 70% and to the category 'mixed' otherwise, as done by Breidenbach et al. (2008) and Latifi et al. (2012). Other thresholds were not explored in this study, even though they may also have an impact on model performance (Hill et al. 2018). However, this study was not focused on the investigation of categorical variables, as categorical variables have the disadvantage of requiring an additional degree of freedom for each level. This effect is amplified when interaction terms between the FTV and other auxiliary variables are included in the model. This is particularly problematic when the number of sample-plots is small, as in this study. A rule of thumb says that 10–20 observations per auxiliary variable are required to be able to detect reasonable-sized effects with reasonable power (Harrell, 2017).

### 2.5.3 Forest type variable *ground_proportion* and classification accuracy

FTVs derived from FTMs (section 2.5.2) are usually not error free, as shown, for example, by Hill et al. (2018) and Straub et al. (2009). We evaluated classification accuracy to understand the precision and the errors of the different FTVs and FTMs. This was done by evaluating the correlation of the continuous FTVs *area_prop*, *area_chm_prop* and *area_chm_sq_prop* with *ground_proportion* (Figure 7). *ground_proportion* represented the conifer timber volume proportion for each sample-plot based on field measurements. This variable was derived

381 from the volumes of the individual trees, which were predicted by means of the volume
382 functions with DBH as an input variable (see section 2.4). *ground_proportion* was not an
383 error-free variable, since the underlying volume functions were not error free, but field
384 measurements are usually more precise than variables derived from remote sensing data.

385 The analyses showed that the LiDAR-derived FTVs had the strongest correlation with
386 *ground_proportion* for all study areas. The FTVs *area_chm_sq_prop* and *area_chm_prop*
387 were more reliable than *area_prop*, except for the FTMs Sen and DLT, which had low
388 resolutions of 10 m and 20 m, respectively. The classification accuracy generally increased
389 with average canopy height in the sample-plot. Therefore, including an interaction term
390 between the FTVs and *MEAN* had the potential to further improve model accuracy, and it
391 was considered in some model formulations. To explore the potential benefit of having a
392 highly precise FTM (i.e. without classification error) based on field measurements, we
393 considered *ground_proportion* as a FTV in our statistical models. Although classification
394 errors of forest type are typically small when they are based on accurate field observations,
395 the *ground_proportion* FTV used in our study was not error free because its derivation was
396 based on volume estimations from volume functions.

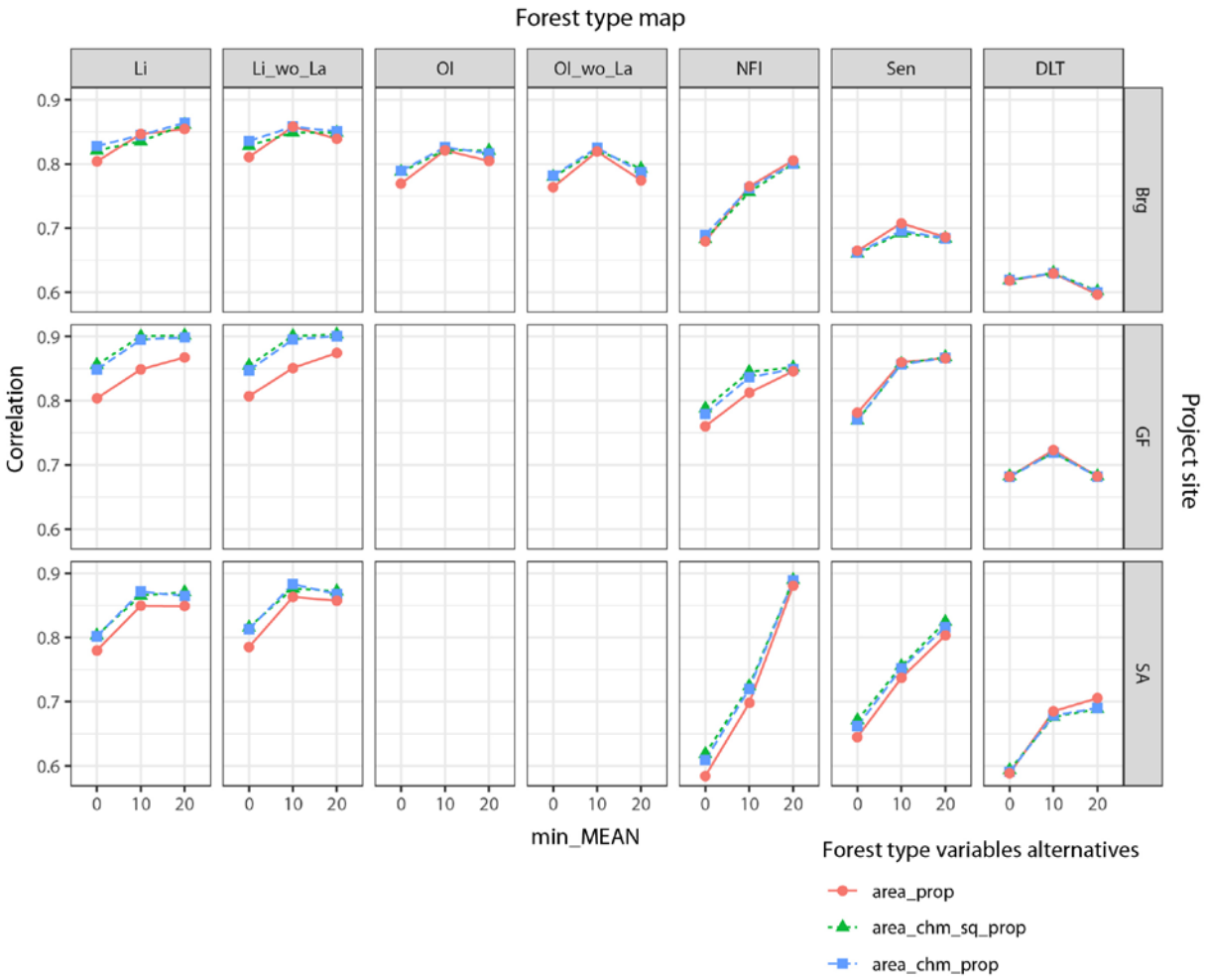


**Figure 7: Correlation of the proportion of conifer timber volume, derived using the different FTMs and FTV alternatives compared with the variable *ground_proportion*. The figure is separated into different average classes of the CHM that were considered. min_MEAN = 20 means that only sample-plots with a minimum average canopy height of 20 m were considered; a value of 0 means that all sample-plots were considered for the analysis of the correlation. Brg = Bremgarten, GF = Glâne-Farzin (GF) and SA = Sarine.**

## 2.6 Statistical methods

For model building, we excluded sample-plots with a timber volume value of zero and sample-plots in which harvests had taken place in the period between the field measurements and the acquisition of the remote sensing data. This step is referred to as 'cleaning' in Table 1. The FTMs derived from orthoimage (OI) and LiDAR (Li) differentiated between deciduous and evergreen foliage. To differentiate accurately between conifer and broadleaf trees for these FTMs, we removed sample-plots that include larch (*Larix decidua*). We labelled these cases with the suffix 'wo_La' (without larch). The number of remaining

411 sample-plots in each study area is listed in Table 1. Each FTM, except OI, was tested in all
412 study areas. The abbreviations of all study area and FTM combinations are given in Table 4.

| | Orthoimage (OI) | Swiss NFI Orthoimage (NFI) | Sentinel NFI (Sen) | LiDAR (return intensity) (Li) | Copernicus Dominant Leaf Type (DLT) |
|---|---|---|---|---|---|
| Glâne-Farzin | - | GF_NFI | GF_Sen | GF_Li / GF_Li_wo_La | GF_DLT |
| Sarine | - | SA_NFI | SA_Sen | SA_Li / SA_Li_wo_La | SA_DLT |
| Bremgarten | Brg_OI / Brg_OI_wo_La | Brg_NFI | Brg_Sen | Brg_Li / Brg_Li_wo_La | Brg_DLT |

413 **Table 4: Combinations of study areas and FTMs considered in the statistical analyses.**

414 Root mean square error (RMSE) from leave-one-out cross-validation (LOOCV) was used to
415 denote model accuracy (Equation 1). Table 5 lists the multiple linear regression models used
416 in this study, as basic formulations without FTVs. Each basic formulation was combined with
417 each FTV alternative. To evaluate the gain in model performance when any forest type
418 information was included, each basic formulation with no FTVs was analysed. The statistical
419 software R (version 3.5) was used for model analyses (R Core Team, 2018).

420 $$\boldsymbol{RMSE} = \sqrt{\frac{\sum_{x \in s}\left(\hat{Y}(x) - Y(x)\right)^2}{n}} \qquad \text{(Equation 1)}$$

421 where $Y(x)$ is the observed local density of the timber volume on the sample-plot level at
422 location *x* $x \epsilon (s)$ [$m^3$ $ha^{-1}$], $\hat{Y}(x)$ is the predicted volume density on the sample-plot level at
423 location *x* $x \epsilon (s)$ [$m^3$ $ha^{-1}$], and *s* is the modelling dataset composed of *n* sample-plots.

424 The results are discussed in terms of the relative RMSE, defined as the RMSE relative to the
425 mean $y_{mean}$ of the observed values (Equation 2).

426 $$RMSE[\%] = \frac{RMSE}{y_{mean}} * 100 \text{ , with } y_{mean} = \frac{1}{n}\sum_{x \in s} Y(x) \qquad \text{(Equation 2)}$$

427 The OLS regression model formulation is defined in Equation 3

$$Y(x) = \beta_0 + \beta_1 Z_1 + \beta_2 Z_2 + .. + \beta_p Z_p + \varepsilon(Z) \qquad \text{(Equation 3)}$$

with error term $\varepsilon(Z)$ independent and identically distributed, $E\big(\varepsilon(Z)\big) = 0$, and $Var\big(\varepsilon(Z)\big) = \sigma^2$,

where $Y(x)$ is the response (see Equation 1), $\beta_0 .. \beta_p$ are the regression coefficients, $Z_1 .. Z_p$ denote the auxiliary variables, and *p* is the number of auxiliary variables (explanatory or predictor variables). All models are displayed using the following R-style formatting: $Y \sim Z_1 + Z_2 + .. + Z_p$ (see Table 5).

| Model # | Basic formulation |
|---|---|
| 1 | `VOL ~ MEAN` |
| 2 | `VOL ~ MEAN + STD` |
| 3 | `VOL ~ MEAN + STD + C02` |
| 4 | `VOL ~ MEAN + STD + P90 + C30` |
| 5 | `VOL ~ MEAN + STD + C30 + C02` |
| 6 | `VOL ~ MEAN + STD + C30 + C02 + MEAN:STD` |
| 7 | The model variables were selected based on the Akaike Information Criterion (AIC; Akaike, 2011). All variables from Table 3, such as *MEAN, STD, CXX* and *PXX*, were available for selection. The selected variables are listed in Table A1 in the Appendix. |
| 8 | Same variables as Model #7, but with the following interaction terms:<br>`MEAN + MEAN:STD + (MEAN:foresttype) + (MEAN^2:foresttype)`<br>After adding the interaction terms, variable selection based on the AIC was again performed (for each forest type alternative) |
| 9 | Same variables as #7, but with the following interaction terms:<br>`MEAN + MEAN:STD + (MEAN:foresttype) + (MEAN^2:foresttype)` |
| 10 | `VOL ~ MEAN + STD + MEAN:STD`<br>For the forest types with the following interaction terms:<br>`foresttype + (MEAN:foresttype)+(MEAN^2:foresttype)`<br>variable selection based on the AIC was performed (for each forest type alternative) |
| 11 | `VOL ~ MEAN + STD + MEAN:STD`<br>For the forest types with the following interaction terms: `foresttype + (MEAN:foresttype)+(MEAN^2:foresttype)`<br>(same variables as #10, but without AIC variable selection) |

**Table 5: Basic model formulations for the multiple linear regression. The interaction terms are indicated by':'. 'foresttype' stands for the forest type variable and is either *area_prop*, *area_chm_prop*, *area_chm_prop*, *categorical* or *ground_proportion*.**

Models 1–5 were quite simply models without interaction terms (Table 5). Model 6 included the interaction between *MEAN* and *STD*. Model 7 was evaluated by performing variable selection based on the Akaike Information Criterion (AIC; Akaike, 2011). Models 8 and 9 included further interaction terms. For Model 8, variable selection (based on AIC) was performed a second time after the interaction terms were added. Models 10 and 11 had

443 only three variables but included interaction terms. Variable selection (based on AIC) was
444 performed to find a satisfactory relationship between the goodness of fit and the simplicity
445 of the model in Model 10 but not in Model 11. The formulations for the best performing
446 model (Model 10) are given in Table 7.

447 We additionally computed the adjusted coefficient of determination (adjusted r-squared) to
448 facilitate comparisons with other related publications. The adjusted r-squared values were of
449 limited use for the evaluation of the models, as over-fitted models, such as Models 9 and 11,
450 also had high adjusted r-squared values. Models with many variables are generally at risk of
451 over-fitting. Therefore, cross-validation with RMSE % was considered better suited for the
452 evaluation of our OLS regression models. We did not evaluate results based on the adjusted
453 r-squared values, but these values can be found in the Appendix (Figures A1 and A2).

454 # 3 Results

455 ## 3.1 Bremgarten (Brg)

456 The results of the leave-one-out cross-validation (LOOCV) (RMSE %) are depicted in Figure 8,
457 which shows the accuracies of the OLS regression models, defined in Table 5, achieved for
458 models including all combinations of the four different FTV alternatives and without FTVs
459 ('None').

460 Including the FTM information substantially reduced the cross-validated RMSE for all
461 models. The best model performance (lowest RMSE) for all FTMs was reached with Model 8
462 (Figure 8), where a double stepwise selection procedure was applied that also allowed
463 interaction terms to remain in the model. The best model performance was achieved by
464 adding FTVs based on the LiDAR dataset (Brg_Li and Brg_Li_wo_La). The reduction in RMSE
465 was up to 9 percentage points in comparison to models without any FTM information (Figure
466 9). Further, the FTV alternative influenced the accuracy of the model. The FTV alternatives

467 *area_chm_sq_prop* and *area_chm_prop* showed similar results and performed better than
468 *area_prop*, which in turn outperformed the categorical variable. It is quite remarkable that
469 models including the FTV alternatives *area_chm_sq_prop* and *area_chm_prop* derived from
470 LiDAR data outperformed the model with *ground_proportion* (conifer timber volume
471 proportion, derived from field measurements). Model performance improved further when
472 inventory sample-plots with larch were excluded (Brg_Li_wo_La; Figure 8).

473 The FTVs derived from the orthoimages (Brg_NFI, Brg_OI and Brg_OI_wo_La) reduced the
474 RMSE by 4–6 percentage points in comparison to models without any FTM information (e.g.
475 from 45% to 39% for Model 1 in Brg_NFI). Whereas almost no difference could be observed
476 among models including the different FTV alternatives for Brg_NFI, slight differences existed
477 among the models depending on the FTV alternative included for Brg_OI and Brg_OI_wo_La,
478 which were based on a 2 m x 2 m orthoimage. Models based on Sentinel data (Brg_Sen)
479 showed slightly higher RMSE values compared with those derived from orthoimages. The
480 lowest model accuracy was achieved by incorporating FTVs derived from the DLT FTM, with
481 a model improvement of only of 1–2 percentage points.

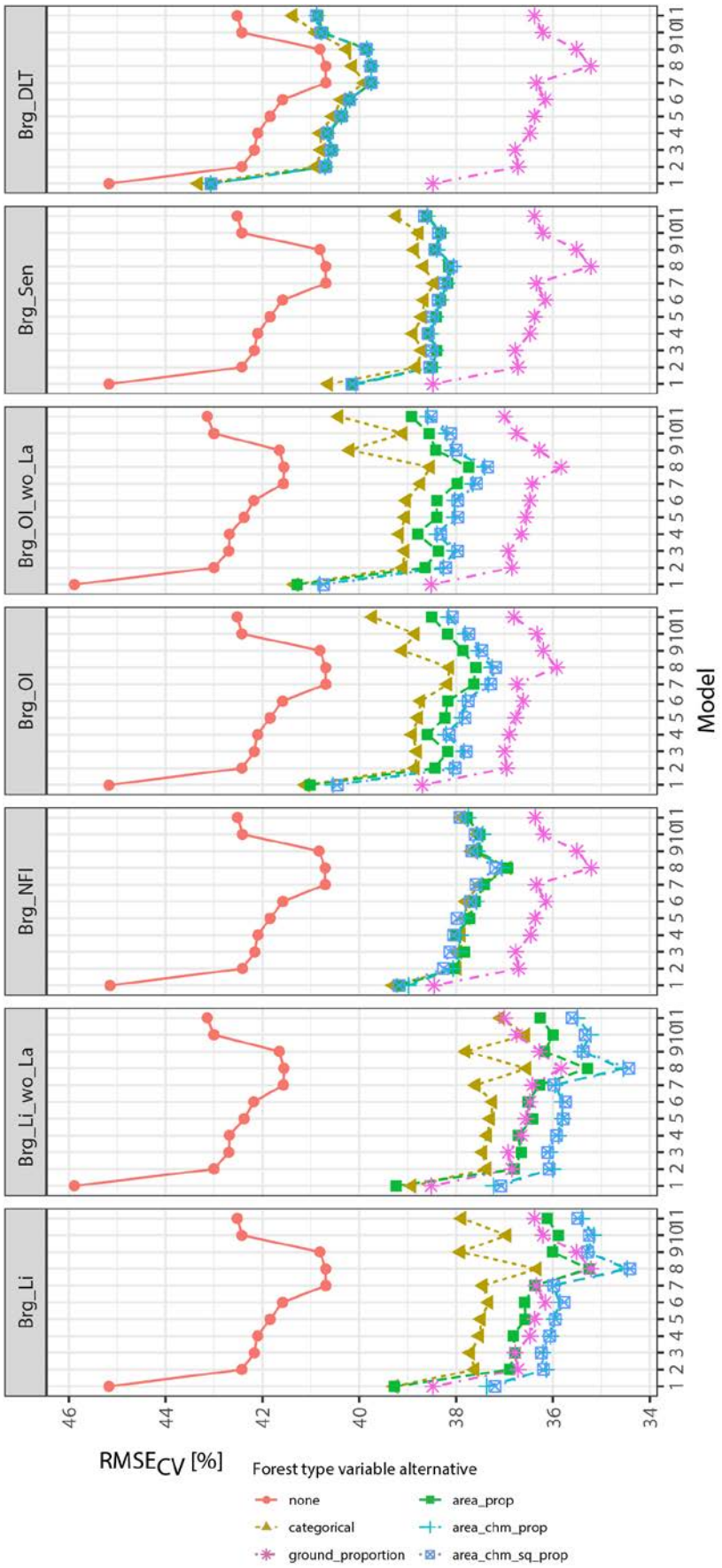


482

483 **Figure 8: Leave-one-out cross-validated RMSE$_{CV}$ [%] for each regression model, FTM and combination of FTV**
484 **alternatives in the case study area Bremgarten (Brg).**

## 3.2 Glâne-Farzin and Sarine

When interpreting the results of GF and SA, it should be kept in mind that the positional accuracy of the sample-plot centres is less precise (Table 1). Thus, we expected smaller improvements in model accuracy by adding FTVs. The RMSE values for GF and SA are presented in Figure 10. Like in Brg, Model 8 achieved the lowest RMSE overall, and for SA_Li Model 10 was equivalent to Model 8. The largest model improvement was reached by adding the LiDAR based FTVs (SA_Li and SA_Li_wo_La) to the regression models and by using the FTV alternatives *area_chm_sq_prop* and *area_chm_prop*. Including these variables led to better model performance than when *ground_proportion* was included. The gain in model accuracy was more than 2.5 percentage points (Model 10; Figure 9). Auxiliary variable combinations of the remaining FTMs (SA_NFI, SA_Sen and SA_DLT) showed similar patterns and reduced the RMSE by about 1–2 percentage points. Comparing the results of GF with the other study areas, the RMSE without FTVs was already lower (RMSE ≈ 32%, Figure 10) than the RMSE of the best models containing FTVs in Brg (RMSE ≈ 34%) or SA (RMSE ≈ 36%).

Including forest type information in the regression models led to an improvement in model performance (Figure 10). FTVs derived from the LiDAR FTM showed again the lowest RMSE values. In comparison to the other study areas, including FTVs had a smaller effect on model accuracy for GF. In some cases the categorical variable performed best (GF_Li) by a very small margin. However, including FTM information in the model resulted in a decrease in RMSE in the best case ($RMSE_{CV}$ ≈ 28% for Model 8 and GF_Li_wo_La; Figure 10). Contrary to results for SA and Brg, including *ground_proportion* as a predictor resulted in a slightly better model performance than using FTVs from maps. GF was the study area with the smallest number of sample-plots; for this reason, GF had the highest risk of model over-fitting among the three study areas, and over-fitting was also detected for the combination of Models 7–9,

509 FTM Li_wo_La and without FTV. The adjusted r-squared values (Figure A2 in the Appendix)
510 indicate an excellent model performance (high adjusted r-squared value), whereas the high
511 $RMSE_{CV}$ value in Figure 10 indicates the opposite. However, this was the only case of over-
512 fitting. A further comparison of adjusted r-squared values (Figure A2) demonstrates that the
513 remaining models with the highest adjusted r-squared values (Model 9 and GF_Li_wo_La)
514 had rather low RMSE values.

515 Table 6 shows the model formulations for the best performing models. Although some
516 models had many predictors, they were not over-fitted, as shown through the leave-one-out
517 cross-validated RMSE (Figures 8 and 10). For Brg and SA, Model 10 provided the second best
518 model performance according to RMSE, which was only slightly worse than that of Model 8
519 (Table 7) but included far fewer variables.

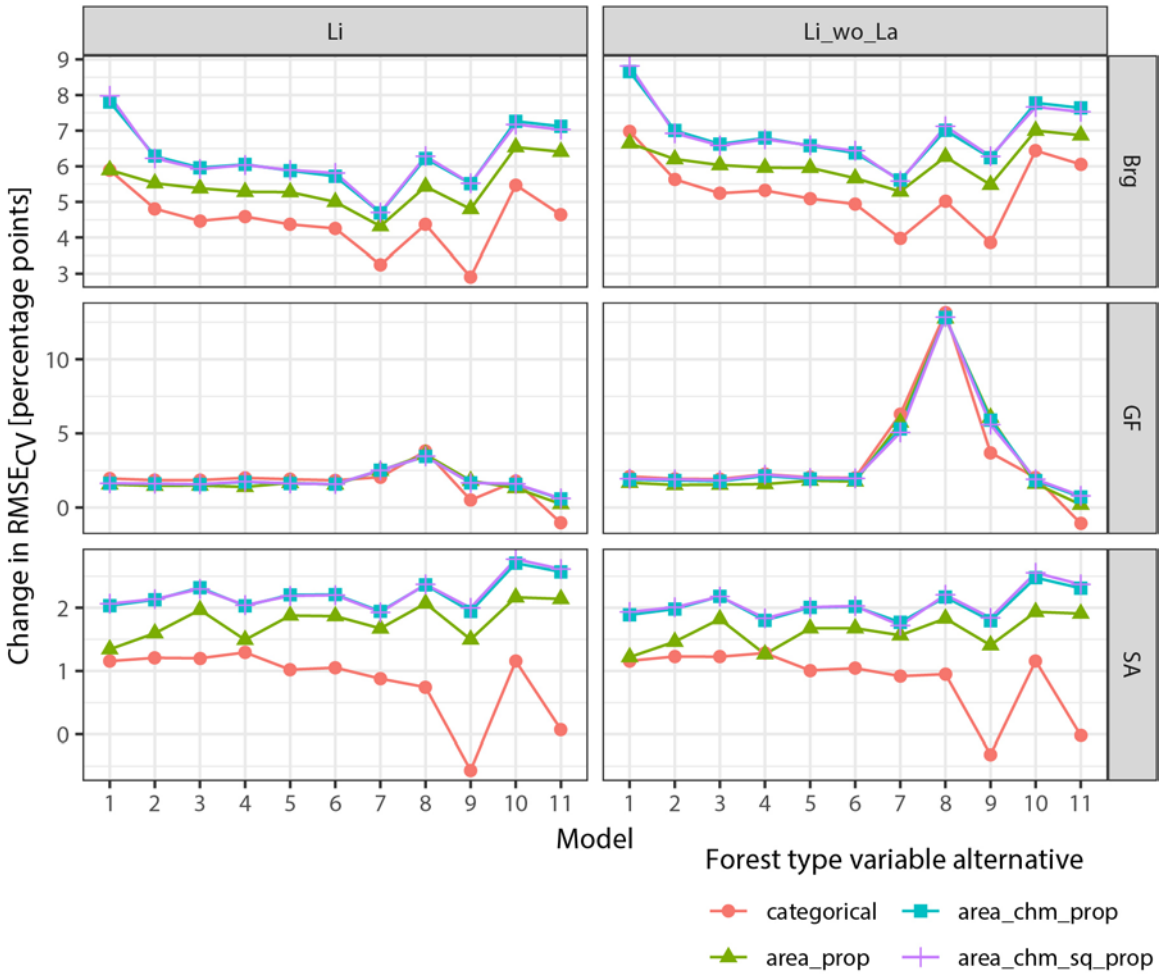


520

521 **Figure 9: Change in $RMSE_{CV}$ [%] values under the different model types and forest type variables (FTV)**
522 **alternatives compared with a model without FTVs in the three case study areas (Brg = Bremgarten, GF =**
523 **Glâne-Farzin, SA = Sarine). Results are only displayed for variables derived from the LiDAR FTM. The peak in**
524 **GF and Li_wo_La for Models 7–9 was caused by over-fitted models without FTVs.**

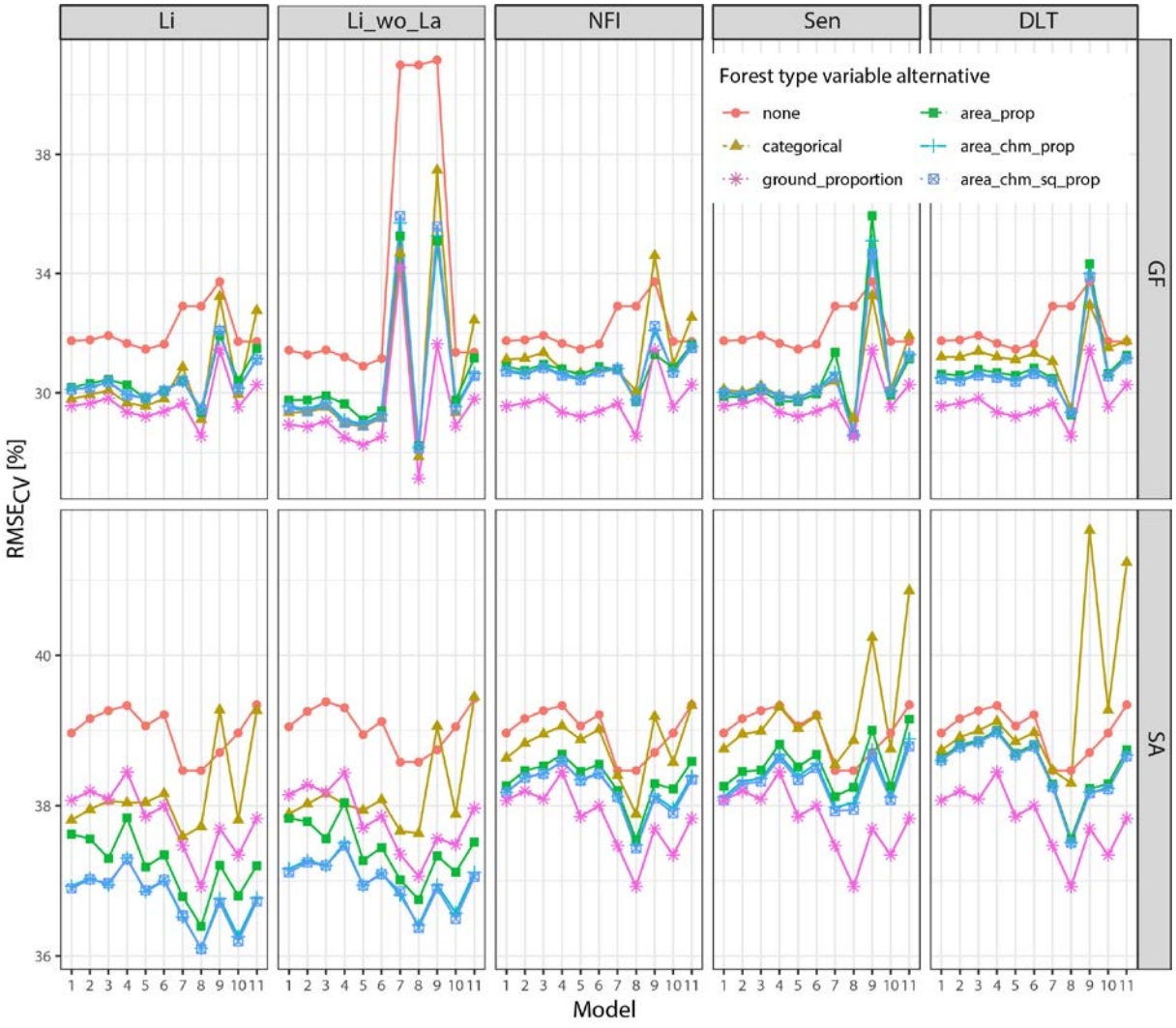


**Figure 10: Leave-one-out cross-validated $RMSE_{CV}$ [%] for each regression model, forest type map and combination of forest type variable alternatives in the case study areas Glâne-Farzin (GF) and Sarine (SA).**

| Study area | Model | Forest type variable | Auxiliary variables used |
|---|---|---|---|
| Brg_Li | 8 | area_chm_sq_prop | P40 + P30 + P25 + P01 + C10 + C20 + foresttype + MEAN + foresttype:MEAN |
| Brg_Li | 8 | area_chm_prop | P40 + P30 + P25 + P01 + C10 + C20 + foresttype + MEAN + foresttype:MEAN |
| Brg_Li_wo_La | 8 | area_chm_sq_prop | P99 + P60 + P01 + C10 + C20 + CV + foresttype + MEAN + foresttype:MEAN |
| Brg_Li_wo_La | 8 | area_chm_prop | P99 + P60 + P50 + P30 + P01 + C10 + C20 + CV + foresttype + MEAN + foresttype:MEAN |
| GF_Li | 8 | categorical | P60 + P25 + C02 + C10 + C15 + C25 + C30 + foresttype + MEAN |
| GF_Li_wo_La | 8 | categorical | C02 + C10 + C15 + C25 + C30 + foresttype + MEAN + foresttype:MEAN |
| SA_Li | 8 | area_chm_sq_prop | P20 + C05 + C15 + C20 + C25 + C35 + C50 + foresttype + MEAN + foresttype:MEAN |

| | | | |
|---|---|---|---|
| SA_Li | 8 | area_chm_prop | P20 + C05 + C15 + C20 + C25 + C35 + C50 + foresttype + MEAN + foresttype:MEAN |
| SA_Li_wo_La | 8 | area_chm_sq_prop | MSSq + P25 + P05 + C02 + C15 + C20 + C25 + C35 + C50 + chm_sq_average + foresttype + MEAN + foresttype:MEAN |
| SA_Li_wo_La | 8 | area_chm_prop | MSSq + P25 + P05 + C02 + C15 + C20 + C25 + C35 + C50 + chm_sq_average + foresttype + MEAN + foresttype:MEAN |

**Table 6: Selected model formulations for the best performing forest type model combinations for Model 8. Interaction terms are indicated by ':'. 'foresttype' stands for the forest type variable and is either *area_prop*, *area_chm_prop*, *area_chm_prop*, *categorical* or *ground_proportion.***

| Study area | Model | Forest type variable | Auxiliary variables used |
|---|---|---|---|
| Brg_Li | 10 | area_chm_sq_prop | MEAN + STD + foresttype + MEAN:foresttype |
| Brg_Li | 10 | area_chm_prop | MEAN + STD + foresttype + MEAN:foresttype |
| Brg_Li_wo_La | 10 | area_chm_sq_prop | MEAN + STD + foresttype + MEAN:foresttype |
| Brg_Li_wo_La | 10 | area_chm_prop | MEAN + STD + foresttype + MEAN:foresttype |
| GF_Li | 10 | categorical | MEAN + STD + foresttype + MEAN:STD |
| GF_Li_wo_La | 10 | categorical | MEAN + foresttype |
| SA_Li | 10 | area_chm_sq_prop | MEAN + foresttype + MEAN:foresttype |
| SA_Li | 10 | area_chm_prop | MEAN + foresttype + MEAN:foresttype |
| SA_Li_wo_La | 10 | area_chm_sq_prop | MEAN + foresttype + MEAN:foresttype |
| SA_Li_wo_La | 10 | area_chm_prop | MEAN + foresttype + MEAN:foresttype |

**Table 7: Selected model formulations for the best performing forest type model combinations for Model 10. Interaction terms are indicated by ':'. 'foresttype' stands for the forest type variable and is either *area_prop*, *area_chm_prop*, *area_chm_prop*, *categorical* or *ground_proportion.***

# 4 Discussion

## 4.1 Influence of different forest type variables and forest type maps on model performance

Our results confirm the findings of previous studies (Breidenbach et al., 2008; Latifi et al., 2012) that incorporated FTM information to predict timber volume. Both earlier studies reported an increase in model accuracy (measured as the LOOCV RMSE) of the OLS regression models for their investigated study areas. In doing so, Latifi et al. (2012) found an improvement of 2–4 percentage points in RMSE when stratifying into broadleaf and conifer

543 forest types. We found similar improvements when the categorical FTV was included in
544 models (Figure 9). In our study, the best performing FTM in all study areas was the one
545 derived from leaf-off LiDAR data. This is not particularly surprising, as this map had both the
546 highest resolution and the best correlation with the values derived from field measurements
547 (*ground_proportion*), as visualized in Figure 7. The further order of the best suited FTMs was
548 less clear and varied between the study areas. In general, a map with a higher resolution
549 gave better results than one with a coarser resolution, even if both maps showed the same
550 classification accuracy, as derived in section 2.5.3. This was observed in Brg (Figure 8), where
551 we had the following order of accuracy according to the RMSE: Brg_OI (2 m x 2 m) ≈ Brg_NFI
552 (3 m x 3 m) > Brg_Sen (10 m x 10 m) > Brg_DLT (20 m x 20 m). The NFI Orthoimage map
553 (*_NFI) is biased due to topographic and illumination effects, i.e. shadows, of optical remote
554 sensing data (Waser et al., 2017).

555 We found that the selection of a FTV alternative strongly affected model accuracy,
556 particularly when FTMs with a high resolution (≤ 2 m) were used, such as the LiDAR-derived
557 map (0.5 m). The continuous variables thus outperformed the categorical variable. Among
558 the continuous variables, *area_chm_prop* and *area_chm_sq_prop* performed about equal
559 and were associated with higher model accuracies than *area_prop*. For *area_chm_prop* and
560 *area_chm_sq_prop*, the forest type proportion was weighted by canopy height information
561 of a CHM. This representation mapped the volume proportions of conifers and broadleaf
562 trees better, in particular for mixed and heterogeneously structured forests. The difference
563 in RMSE between all the different FTV alternatives was up to 2 percentage points. However,
564 in GF there was no clear difference between the different FTV alternatives, possibly because
565 exactly georeferenced sample-plot positions were not available and the model accuracy was
566 already high without incorporating FTVs (Figure 9). The gain in model accuracy was up to 9

RMSE percentage points for Brg, and up to 3 percentage points for GF and SA. The improvement in model accuracy, measured as percentage points of the RMSE, was lower in GF and SA compared with Brg, as the results from GF and SA already showed a small RMSE before any forest type information was added to the OLS regression model.

## 4.2 Best performing model formulation

Our second research question was how to best include FTM information in a regression model. Model 8 performed best for all study areas and FTV combinations. This model was calibrated using a variable selection procedure based on AIC values, followed by the addition of interaction terms, and finally a second variable selection based on AIC values. Except for GF_Li, all of the best performing models included an interaction term between *foresttype* and *MEAN* (Table 6). Therefore, we highly recommend using interaction terms when including FTM information in OLS regression models. Interaction terms are particularly meaningful because, depending on the average vegetation height, the FTMs have a different classification accuracy (Figure 7).

Although Model 8 included several variables, over-fitting was not an issue, as shown by the cross-validation results. However, if we were interested in making inferences about the predictors, Model 8 could have failed. In such cases, Model 10 would have been the preferred model formulation because it included remarkably fewer variables (Table 7). Due to its smaller number of variables, Model 10 was also less vulnerable to over-fitting. Further, variance inflation, which occurs as a consequence of including too many correlated variables and is quantified as the variance inflation factor (VIF), could affect the significance of single variables (Fox and Monette, 1992). This was not the case in our study, however, because Model 10 had the best AIC and highly correlated variables were eliminated. The only issue could be that main effects are difficult to interpret in models with interactions.

## 4.3 Potential of a high-precision forest type variable

The idea behind introducing *ground_proportion* (conifer volume proportion based on field measurements) as a FTV in the models was to explore the potential benefit of having a high-precision FTM without misclassifications. Results from the two study areas Brg and SA show that when the LiDAR-derived FTM is used in combination with the variables *area_chm_prop* and *area_chm_sq_prop*, regression model performance can be even better than when this FTM is used in combination with *ground_proportion*. This result is remarkable and deserves an in-depth discussion. The following issues are relevant for its understanding and interpretation.

First of all, it must be emphasized that both the variable *ground_proportion* and the remote-sensing-based FTV contained errors. In the case of *ground_proportion*, the errors were caused by the volume functions used, which were solely based on the DBH. For example, Kaufmann (2001) explored volume functions for the Swiss NFI. He stated that a tree in a later stage of development has a larger stem volume than a tree with the same DBH in an earlier developmental stage. This behaviour was ignored in the volume functions, but we think that this relationship was mapped in the LiDAR-based 'weighted-canopy-height proportion' FTV, as the canopy height is correlated with the developmental stage of a tree. In the case of the remote-sensing-based FTV, the most relevant sources of error were misclassification (confusion of conifer and broadleaf), inadequate temporal synchronization (a time difference between the field measurements and the recording of remote sensing data), and imperfect spatial matching of the sample-plot location with the detail of the remote sensing data.

Second, the variables *ground_proportion* and *area_chm_prop* / *area_chm_sq_prop* can only be compared directly if they are derived identically. This would be the case if

615 *ground_proportion* was also derived by weighting the broadleaf/conifer sample tree
616 information by the respective tree heights – analogous to calculating *area_chm_prop* /
617 *area_chm_sq_prop*. However, this was not the case because tree heights were not recorded.
618 Third, the response variable, the volume per sample-plot, which was calculated by the same
619 volume functions as used to derive the forest type proportion (*ground_proportion*), was also
620 not error free and contains the same errors as the field observed FTV. The applied volume
621 functions ignore some real-existing influences on the tree volume and they therefore return
622 the same volume for different values of some influential factors. The evaluation and
623 comparison of different models and auxiliary variables is therefore always limited by the
624 accuracy of the reference values, which were in our case generated by one-parameter
625 volume functions. In order to allow a more precise interpretation of the results, one would
626 have to use more precise, e.g. three-parameter volume functions. Therefore, it is difficult to
627 say whether there was actually a statistically significant difference between the results
628 obtained by ground based forest type information and remote sensing based forest type
629 information.
630 Overall, the following conclusions can be drawn: (1) Although the FTM-based variables are
631 error prone, they can generate a more powerful signal for modelling than the field based
632 information *ground_proportion*. This supports the statement that the proposed weighting by
633 canopy height information of the FTV generates a very useful signal.
634 (2) Until now, it has always been assumed that field information is the reference in terms of
635 accuracy. However, this concept is limited by the sampling protocol; in this case, no tree
636 heights were measured during the field observation and therefore the corresponding
637 calculation of ground reference including tree height information was not possible. If tree

height had been recorded, the ground reference would possibly have been as good or better than the FTM-based variables.

Nevertheless, we recommend including *ground_proportion* as a FTV in regression models, particularly during model evaluation, because the variable might serve as a benchmark to assess the effect of including FTM information. Additionally, it might function as an indicator of whether it is worth investing resources into creating an advanced FTM.

## 4.4 Generalization of the Results

In order to address our second research question, we studied the effect of incorporating different FTV alternatives in three independent study areas. We considered the results in Brg, with its precisely measured forest inventory sample-plots, as the reference. The main findings were that the best results were generally achieved: (1) by deriving forest type variables from a FTM with a high resolution and (2) by concurrently using forest type variables, such as *area_chm_prop* and *area_chm_sq_prop*, derived by a superimposed evaluation of the FTM and the CHM. These findings apply to Brg and SA. For GF, point (2) could not be confirmed, on the one hand because the terrestrial inventory sample-plot centres were not positioned accurately and on the other hand because GF is less heterogeneously structured than the other forests because it is dominated by numerous pure mature conifer sample-plots (Figure 3). To summarize, precisely measured inventory sample-plots and the presence of mixed and heterogeneously structured forests are required for this approach to be beneficial for current inventories. Further, leaf-off LiDAR data is desirable. We worked with a LiDAR data density of 8 and 10 points $m^{-2}$, which delivered excellent results. Such data is widely available; for example, by 2023 Switzerland will be covered completely with leaf-off LiDAR data with an average density of 15–20 points $m^{-2}$.

## 4.5 Relevance for management

Climate change is expected to considerably influence forest ecosystems and their management (Hanewinkel et al., 2013; Schelhaas et al., 2015). In combination with climate change, disturbances are expected to increase and affect forest ecosystems (Seidl et al., 2017, 2014). To face these future challenges, Messier et al. (2019) recommended using forest management to increase the number of tree species and the structural diversity of forests at the landscape scale to improve the resilience of forests. Managing forests for higher resilience requires, however, more accurate and more spatially explicit information on the current situation of forests, which is usually assessed during forest inventories. Such information is used to guide forest practitioners in their management aims, which further include providing the demanded ecosystem services and the conservation of forest biodiversity in the best possible way (Bäck et al., 2017; MEA, 2005). Assessment of the standing timber volume therefore provides important information to practitioners because management activities are very often addressed primarily in forest stands with the largest timber volumes, as they contain the highest accumulated timber values and require cautious planning of harvesting activities and stand regeneration. Further, the standing timber volume is often used as an important indicator to quantify the provisioning of timber production (Blattert et al., 2017; Bugmann et al., 2017), which is still one of the most important ecosystem services in forestry. Improved inventory fundamentals have further implications. They lead to improved management solutions, such as more efficient harvesting or road network layouts (Bont et al., 2019, 2012), as timber volume is usually a major component used to form such solutions (Bont and Church, 2018). With our presented method for incorporating FTM information, predictions about the standing timber volume

can be provided for forest management with higher accuracy compared with classical approaches and on larger scales.

# 5 Conclusions

We draw the following three major conclusions from our study: (1) Incorporating FTM information into ordinary least squares (OLS) linear regression models for predicting timber volume on the sample-plot level increased model accuracy. An improvement in RMSE of up to 9 percentage points in comparison to models not using any forest type information was observed. The highest explanatory power of regression models was achieved by weighting high-resolution FTM information (leaf-off LiDAR) with superimposed canopy height model (CHM) information. This new approach of deriving FTVs improved the RMSE by up to 2 percentage points compared with classical approaches. (2) The OLS regression models had the best fit when they included an interaction term between mean canopy height and forest type. (3) Considering *ground_proportion* (the value derived from field measurements on the inventory sample-plots) in the model evaluation could serve as an important benchmark and/or upper bound for assessing the improvement in model accuracy when FTM information is included in model definitions.

Overall, our new method of deriving FTVs better reflects timber volume in heterogeneously structured and mixed forests. Detailed standing timber volume assessments are relevant for guiding practitioners in managing forests for multiple ecosystem services, particularly nowadays when resilient forests with a diverse structure and species mixture are needed to face the challenges of climate change. However, further research is required regarding different statistical model types. For example, it would be interesting to know if our findings can be transferred to other modelling approaches. In addition, a detailed differentiation into

single tree species or main tree species, beyond the conifer / broadleaf classification, could be a further development of this new approach.

**Funding:** This research was partially funded by the Swiss Forest and Wood Research Fund (WHFF) (Project 2015.01).

**Acknowledgements:** We thank Pierre Cothereau and Robert Jenni from the Canton of Freiburg for supporting this project. We also thank Dr. Markus Kalisch from the Seminar for Statistics (ETH Zurich) for his practical input concerning statistical analysis, and Melissa Dawes for English editing assistance. We are especially grateful to the WSL, in particular Dr. Oliver Thees and Dr. Renato Lemm, for collaboration and supporting this project. We also thank two anonymous reviewers for their valuable support in improving the manuscript.

**Conflicts of Interest:** The authors declare no conflict of interest and the funding sponsors had no role in the design of the study; in the collection, analyses or interpretation of data; in the writing of the manuscript; or in the decision to publish the results.

# References


Akaike, H., 2011. Akaike's information criterion. International encyclopedia of statistical science 25–25.

Bäck, J., Aszalós, R., Ceulemans, R.J., Glatzel, G., Hanewinkel, M., Kakaras, E., Kotiaho, J.S., Lindroth, A., Lubica, D., Luyssaert, S., 2017. Multi-functionality and sustainability in the European Union's forests. EASAC policy report.

Barrett, F., McRoberts, R.E., Tomppo, E., Cienciala, E., Waser, L.T., 2016. A questionnaire-based review of the operational use of remotely sensed data by national forest inventories. Remote Sensing of Environment 174, 279–289. https://doi.org/10.1016/j.rse.2015.08.029

Blattert, C., Lemm, R., Thees, O., Lexer, M.J., Hanewinkel, M., 2017. Management of ecosystem services in mountain forests: Review of indicators and value functions for model based multi-criteria decision analysis. Ecological Indicators 79, 391–409. https://doi.org/10.1016/j.ecolind.2017.04.025

Bont, L.G., Church, R.L., 2018. Location set-covering inspired models for designing harvesting and cable road layouts. Eur J Forest Res 137, 771–792. https://doi.org/10.1007/s10342-018-1139-7

Bont, L.G., Heinimann, H.R., Church, R.L., 2012. Concurrent optimization of harvesting and road network layouts under steep terrain. Ann Oper Res. https://doi.org/10.1007/s10479-012-1273-4

Bont, L.G., Maurer, S., Breschan, J.R., 2019. Automated Cable Road Layout and Harvesting Planning for Multiple Objectives in Steep Terrain. Forests 10, 687. https://doi.org/10.3390/f10080687

Breidenbach, J., Kublin, E., McGaughey, R.J., Andersen, H.-E., 2008. Mixed-effects models for estimating stand volume by means of small footprint airborne laser scanner data. Photogrammetric Journal of Finland 21, 4–15.

Breiman, L., 2001. Random forests. Machine learning 45, 5–32.

Bugmann, H., Cordonnier, T., Truhetz, H., Lexer, M.J., 2017. Impacts of business-as-usual management on ecosystem services in European mountain ranges under climate change. Reg Environ Change 17, 3–16. https://doi.org/10.1007/s10113-016-1074-4

Eichhorn, F., 2013. Ertragstafeln für die Weißtanne. Springer-Verlag, Berlin, Heidelberg.

ESA, 2019. European Space Agency (ESA), Copernicus Sentinel mission. [WWW Document]. URL https://sentinel.esa.int/web/sentinel/missions

Fassnacht, F.E., Latifi, H., Stereńczak, K., Modzelewska, A., Lefsky, M., Waser, L.T., Straub, C., Ghosh, A., 2016. Review of studies on tree species classification from remotely sensed data. Remote Sensing of Environment 186, 64–87. https://doi.org/10.1016/j.rse.2016.08.013

Fox, J., Monette, G., 1992. Generalized Collinearity Diagnostics. Journal of the American Statistical Association 87, 178–183. https://doi.org/10.1080/01621459.1992.10475190

Gabriel, A., Hill, A., Breschan, J., 2018. Neue Hilfsmittel zur Anwendung zweiphasiger Stichprobenverfahren in der Waldinventurpraxis. Schweizerische Zeitschrift fur Forstwesen 169, 210–219. https://doi.org/10.3188/szf.2018.0210

Hanewinkel, M., Cullmann, D.A., Schelhaas, M.-J., Nabuurs, G.-J., Zimmermann, N.E., 2013. Climate change may cause severe loss in the economic value of European forest land. Nature Clim Change 3, 203–207. https://doi.org/10.1038/nclimate1687

Harrell, F.E., 2017. Regression modeling strategies, Springer Series in Statistics. Springer, Heidelberg.

Hill, A., Buddenbaum, H., Mandallaz, D., 2018. Combining canopy height and tree species map information for large-scale timber volume estimations under strong heterogeneity of auxiliary data and variable sample plot sizes. Eur J Forest Res 137, 489–505. https://doi.org/10.1007/s10342-018-1118-z

Hoffmann, C., 1982. Die Berechnung von Tarifen für die Waldinventur. Forstw Cbl 101, 24–36. https://doi.org/10.1007/BF02741168

Isenburg, M., 2014. Rasterizing Perfect Canopy Height Models from LiDAR. rapidlasso GmbH. URL https://rapidlasso.com/2014/11/04/rasterizing-perfect-canopy-height-models-from-lidar/ (accessed 9.24.19).
Kaufmann, E., 2001. Estimation of Standing Timber Growth and Cut, in: Brassel, P., Lischke, H. (Eds.), Swiss National Forest Inventory: Methods and Models of the Second Assessment. WSL.
Keller, M., 2013. Schweizerisches Landesforstinventar, Feldaufnahme-Anleitung 2013, Internal Report,. WSL, Birmensdorf.
Khosravipour, A., Skidmore, A.K., Isenburg, M., Wang, T., Hussin, Y.A., 2014. Generating Pit-free Canopy Height Models from Airborne Lidar. photogramm eng remote sensing 80, 863–872. https://doi.org/10.14358/PERS.80.9.863
Kukkonen, M., Korhonen, L., Maltamo, M., Suvanto, A., Packalen, P., 2018. How much can airborne laser scanning based forest inventory by tree species benefit from auxiliary optical data? International Journal of Applied Earth Observation and Geoinformation 72, 91–98. https://doi.org/10.1016/j.jag.2018.06.017
Kukkonen, M., Maltamo, M., Korhonen, L., Packalen, P., 2019. Multispectral Airborne LiDAR Data in the Prediction of Boreal Tree Species Composition. IEEE Transactions on Geoscience and Remote Sensing 57, 3462–3471. https://doi.org/10.1109/TGRS.2018.2885057
Lamprecht, S., Hill, A., Stoffels, J., Udelhoven, T., 2017. A Machine Learning Method for Co-Registration and Individual Tree Matching of Forest Inventory and Airborne Laser Scanning Data. Remote Sensing 9, 505. https://doi.org/10.3390/rs9050505
Langanke, T., 2017. Copernicus Land Monitoring Service – High Resolution Layer Forest: Product Specifications Document.
Latifi, H., Fassnacht, F., Koch, B., 2012. Forest structure modeling with combined airborne hyperspectral and LiDAR data. Remote Sensing of Environment 121, 10–25. https://doi.org/10.1016/j.rse.2012.01.015
Liang, X., Hyyppä, J., Matikainen, L., 2007. Deciduous-coniferous tree classification using difference between first and last pulse laser signatures 5.
Magnussen, S., Mandallaz, D., Breidenbach, J., Lanz, A., Ginzler, C., 2014. National forest inventories in the service of small area estimation of stem volume. Can. J. For. Res. 44, 1079–1090. https://doi.org/10.1139/cjfr-2013-0448
Mandallaz, D., 2013. Design-based properties of some small-area estimators in forest inventory with two-phase sampling. Can. J. For. Res. 43, 441–449. https://doi.org/10.1139/cjfr-2012-0381
Mandallaz, D., 2007. Sampling Techniques for Forest Inventories. Chapman and Hall/CRC. https://doi.org/10.1201/9781584889779
Mandallaz, D., Breschan, J., Hill, A., 2013. New regression estimators in forest inventories with two-phase sampling and partially exhaustive information: a design-based Monte Carlo approach with applications to small-area estimation. Can. J. For. Res. 43, 1023–1031. https://doi.org/10.1139/cjfr-2013-0181
McCallum, K., Beaty, M., Mitchell, B., 2014. First Order LIDAR Metrics: A supporting document for LIDAR deliverables. RedCastle Resources Inc., Remote Sensing Applications Center (RSAC), Salt Lake City, Utah.
MEA, 2005. Millennium Ecosystem Assessment - Ecosystems and human well-being. Island press Washington, DC:
Messier, C., Bauhus, J., Doyon, F., Maure, F., Sousa-Silva, R., Nolet, P., Mina, M., Aquilué, N., Fortin, M.-J., Puettmann, K., 2019. The functional complex network approach to foster forest resilience to global changes. For. Ecosyst. 6, 21. https://doi.org/10.1186/s40663-019-0166-2
Næsset, E., 2004. Practical large-scale forest stand inventory using a small-footprint airborne scanning laser. Scandinavian Journal of Forest Research 19, 164–179. https://doi.org/10.1080/02827580310019257
Næsset, E., 2002. Predicting forest stand characteristics with airborne scanning laser using a practical two-stage procedure and field data. Remote Sensing of Environment 80, 88–99. https://doi.org/10.1016/S0034-4257(01)00290-5

824 Ørka, H.O., Næsset, E., Bollandsås, O.M., 2009. Classifying species of individual trees by intensity and
825 structure features derived from airborne laser scanner data. Remote Sensing of Environment
826 113, 1163–1174. https://doi.org/10.1016/j.rse.2009.02.002
827 Packalén, P., Maltamo, M., 2006. Predicting the Plot Volume by Tree Species Using Airborne Laser
828 Scanning and Aerial Photographs. for sci 52, 611–622.
829 https://doi.org/10.1093/forestscience/52.6.611
830 Parkan, M., 2018. Digital Forestry Toolbox for Matlab/Octave.
831 Pretzsch, H., 2001. Modellierung des Waldwachstums. Parey.
832 Pretzsch, H., Biber, P., 2005. A Re-Evaluation of Reineke's Rule and Stand Density Index. for sci 51,
833 304–320. https://doi.org/10.1093/forestscience/51.4.304
834 R Core Team, 2018. R: a language and environment for statistical computing. R Foundation for
835 Statistical Computing, Vienna, Asutria.
836 Räty, J., Vauhkonen, J., Maltamo, M., Tokola, T., 2016. On the potential to predetermine dominant
837 tree species based on sparse-density airborne laser scanning data for improving subsequent
838 predictions of species-specific timber volumes. Forest Ecosystems 3, 1.
839 https://doi.org/10.1186/s40663-016-0060-0
840 Reineke, L.H., 1933. Perfecting a stand-density index for even-aged forests. Journal of Agricultural
841 Research 7, 627–638.
842 Rivoire, M., Le Moguedec, G., 2012. A generalized self-thinning relationship for multi-species and
843 mixed-size forests. Annals of Forest Science 69, 207–219. https://doi.org/10.1007/s13595-
844 011-0158-z
845 Saarela, S., Grafström, A., Ståhl, G., Kangas, A., Holopainen, M., Tuominen, S., Nordkvist, K., Hyyppä,
846 J., 2015. Model-assisted estimation of growing stock volume using different combinations of
847 LiDAR and Landsat data as auxiliary information. Remote Sensing of Environment 158, 431–
848 440. https://doi.org/10.1016/j.rse.2014.11.020
849 Salo, S., Tahvonen, O., 2002. On the Optimality of a Normal Forest with Multiple Land Classes. for sci
850 48, 530–542. https://doi.org/10.1093/forestscience/48.3.530
851 Schelhaas, M.-J., Nabuurs, G.-J., Hengeveld, G., Reyer, C., Hanewinkel, M., Zimmermann, N.E.,
852 Cullmann, D., 2015. Alternative forest management strategies to account for climate change-
853 induced productivity and species suitability changes in Europe. Reg Environ Change 15,
854 1581–1594. https://doi.org/10.1007/s10113-015-0788-z
855 Schmid-Haas, P., 2003. Die Idee der Kontrollstichproben: ihre Entstehung und ihre Zukunft | The
856 Swiss Continuous Forest Inventory: its genesis and its future. Schweizerische Zeitschrift fur
857 Forstwesen 154, 102–111. https://doi.org/10.3188/szf.2003.0102
858 Schmid-Haas, P., Baumann, E., Werner, J., forêt, la neige et le paysage (Birmensdorf) I. fédéral de
859 recherches sur la, 1993. Kontrollstichproben: Aufnahmeinstruktion. Eidgenössische
860 Forschungsanstalt für Wald Schnee und Landschaft.
861 Schweizer, S., 2012. Schweizerischer Forstkalender 2013. Huber, Frauenfeld.
862 Seidl, R., Schelhaas, M.-J., Rammer, W., Verkerk, P.J., 2014. Increasing forest disturbances in Europe
863 and their impact on carbon storage. Nature Climate Change 4, 806–810.
864 https://doi.org/10.1038/nclimate2318
865 Seidl, R., Thom, D., Kautz, M., Martin-Benito, D., Peltoniemi, M., Vacchiano, G., Wild, J., Ascoli, D.,
866 Petr, M., Honkaniemi, J., Lexer, M.J., Trotsiuk, V., Mairota, P., Svoboda, M., Fabrika, M.,
867 Nagel, T.A., Reyer, C.P.O., 2017. Forest disturbances under climate change. Nature Climate
868 Change 7, 395–402. https://doi.org/10.1038/nclimate3303
869 Small, D., 2012. SAR backscatter multitemporal compositing via local resolution weighting, in: 2012
870 IEEE International Geoscience and Remote Sensing Symposium. Presented at the 2012 IEEE
871 International Geoscience and Remote Sensing Symposium, pp. 4521–4524.
872 https://doi.org/10.1109/IGARSS.2012.6350465
873 Steinmann, K., Mandallaz, D., Ginzler, C., Lanz, A., 2013. Small area estimations of proportion of
874 forest and timber volume combining Lidar data and stereo aerial images with terrestrial data.

Scandinavian Journal of Forest Research 28, 373–385. https://doi.org/10.1080/02827581.2012.754936

Straub, C., Dees, M., Weinacker, H., Koch, B., 2009. Using Airborne Laser Scanner Data and CIR Orthophotos to Estimate the Stem Volume of Forest Stands [WWW Document]. URL https://www.ingentaconnect.com/content/schweiz/pfg/2009/00002009/00000003/art00010 (accessed 9.16.19).

Waser, L.T., Ginzler, C., Rehush, N., 2017. Wall-to-Wall Tree Type Mapping from Countrywide Airborne Remote Sensing Surveys. Remote Sensing 9, 766. https://doi.org/10.3390/rs9080766

Xu, Y., Li, C., Sun, Z., Jiang, L., Fang, J., 2019. Tree height explains stand volume of closed-canopy stands: Evidence from forest inventory data of China. Forest Ecology and Management 438, 51–56. https://doi.org/10.1016/j.foreco.2019.01.054

# Appendix

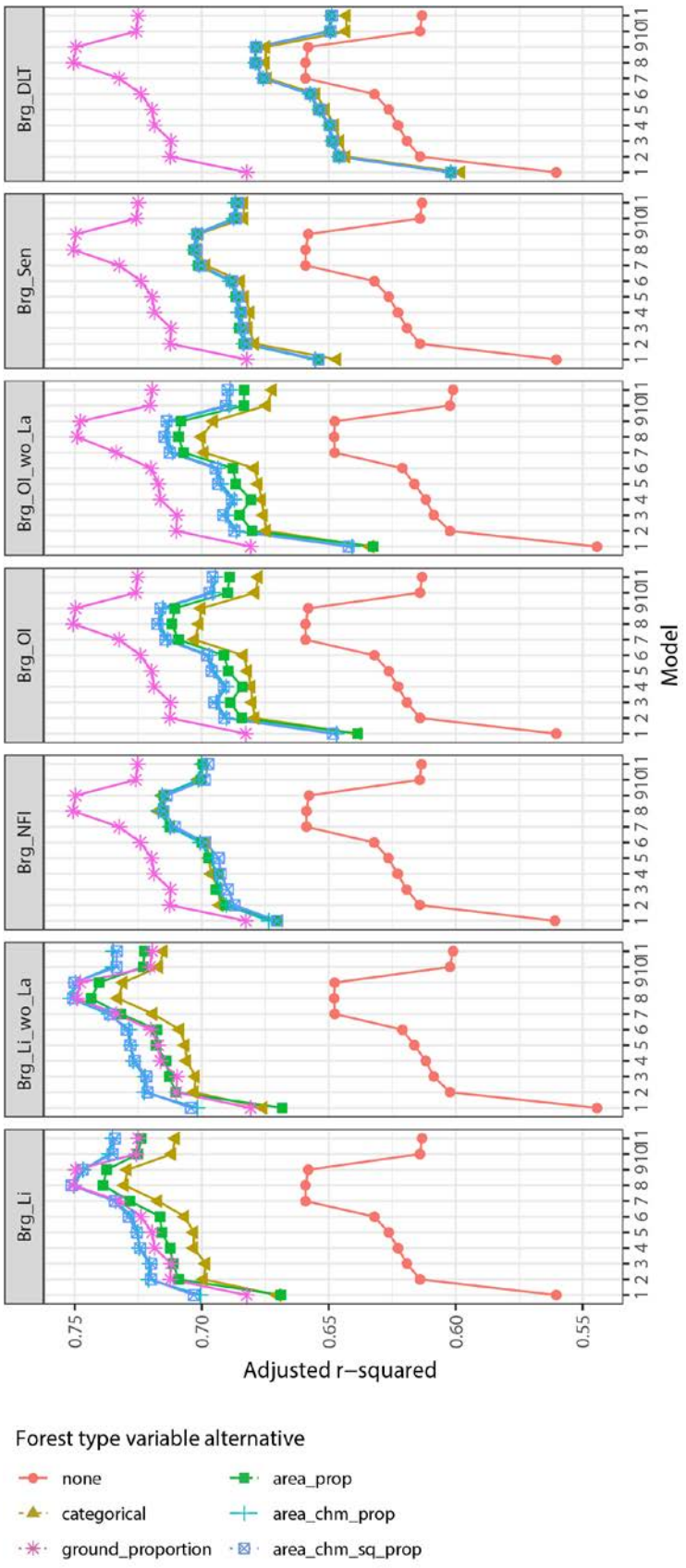


**Figure A1: Adjusted r-squared values for each regression model, forest type map source and combination of forest type variables in the case study area Bremgarten (Brg).**

892

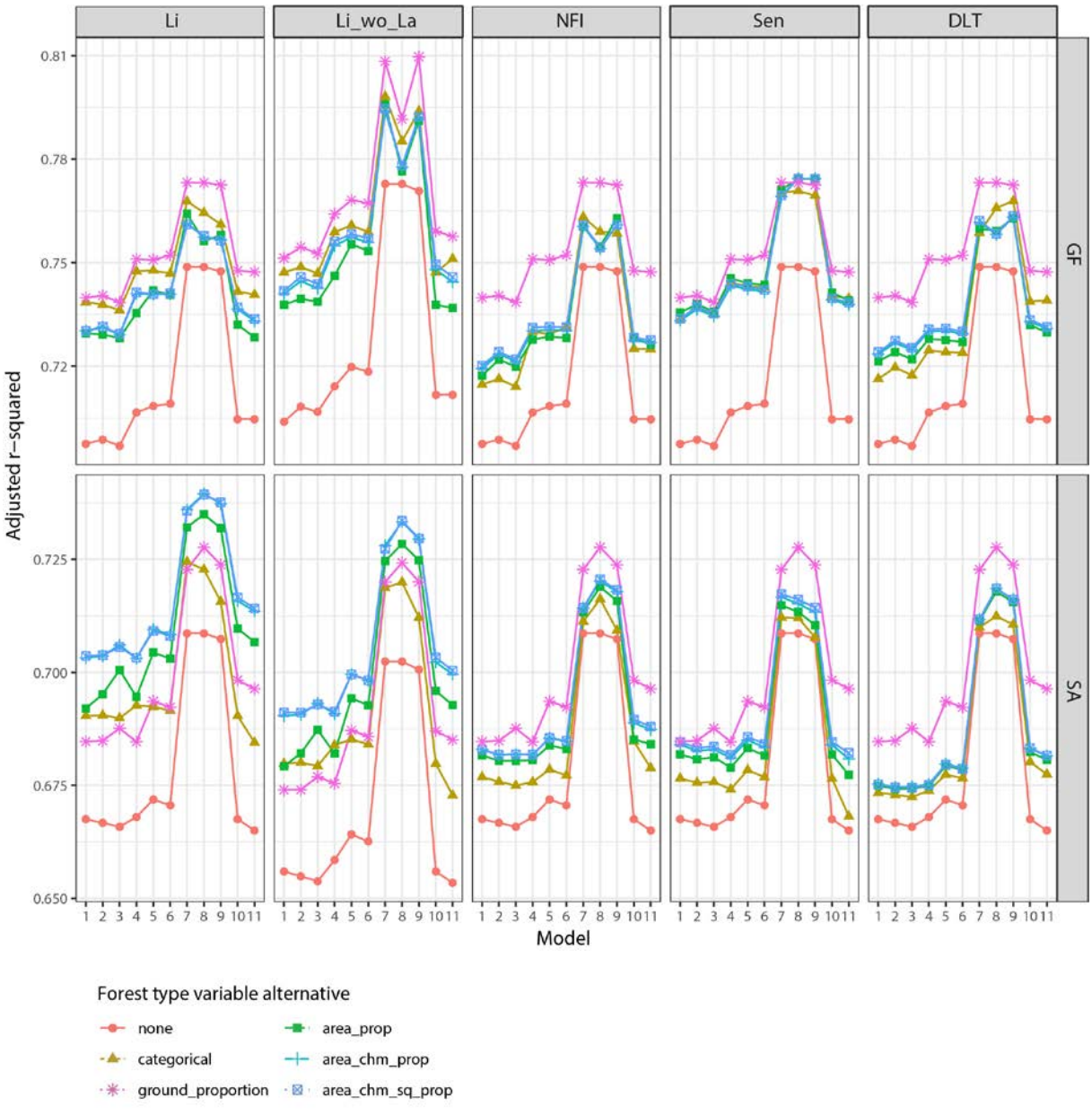


893

894 **Figure A2: Adjusted r-squared values for each regression model, forest type map source and combination of**
895 **forest type variables in the case study areas Glâne-Farzin (GF) and Sarine (SA).**

896

| Study area | Variables |
|---|---|
| Brg_OI | MSSq + STD + MAX + P40 + P30 + P25 + P05 + P01 + C00 + C02 + C10 + C15 + C20 + $MEAN^2$ |
| Brg_OI_wo_La | STD + P99 + P60 + P50 + P30 + P25 + P05 + P01 + C00 + C10 + C20 + CV + STD:MEAN |
| Brg_NFI | MSSq + STD + MAX + P40 + P30 + P25 + P05 + P01 + C00 + C02 + C10 + C15 + C20 + $MEAN^2$ |
| GF_NFI | P95 + P80 + P60 + P40 + P25 + P10 + P01 + C00 + C02 + C05 + C10 + C15 + C20 + C25 + C30 + C35 + C45 + CV |
| SA_NFI | P99 + P95 + P20 + C02 + C05 + C15 + C20 + C25 + C35 + C50 + P60 |
| Brg_DLT | MSSq + STD + MAX + P40 + P30 + P25 + P05 + P01 + C00 + C02 + C10 + C15 + C20 + $MEAN^2$ |
| GF_DLT | P95 + P80 + P60 + P40 + P25 + P10 + P01 + C00 + C02 + C05 + C10 + C15 + C20 + C25 + C30 + C35 + C45 + CV |
| SA_DLT | P99 + P95 + P20 + C02 + C05 + C15 + C20 + C25 + C35 + C50 + P60 |
| Brg_Li | MSSq + STD + MAX + P40 + P30 + P25 + P05 + P01 + C00 + C02 + C10 + C15 + C20 + $MEAN^2$ |
| Brg_Li_wo_La | STD + P99 + P60 + P50 + P30 + P25 + P05 + P01 + C00 + C10 + C20 + CV + STD:MEAN |
| GF_Li | P95 + P80 + P60 + P40 + P25 + P10 + P01 + C00 + C02 + C05 + C10 + C15 + C20 + C25 + C30 + C35 + C45 + CV |
| GF_Li_wo_La | STD + P95 + P80 + P60 + P40 + P30 + P10 + P01 + C00 + C02 + C05 + C10 + C15 + C20 + C45 + $MEAN^2$ |
| SA_Li | P99 + P95 + P20 + C02 + C05 + C15 + C20 + C25 + C35 + C50 + P60 |
| SA_Li_wo_La | MSSq + P25 + P05 + C02 + C05 + C15 + C20 + C25 + C35 + C50 + $MEAN^2$ |
| Brg_Sen | MSSq + STD + MAX + P40 + P30 + P25 + P05 + P01 + C00 + C02 + C10 + C15 + C20 + MEAN2 |
| GF_Sen | P95 + P80 + P60 + P40 + P25 + P10 + P01 + C00 + C02 + C05 + C10 + C15 + C20 + C25 + C30 + C35 + C45 + CV |
| SA_Sen | P99 + P95 + P20 + C02 + C05 + C15 + C20 + C25 + C35 + C50 + P60 |

**Table A1: Selected variables for Model 7. In addition to the listed variables, the FTV can be added (*area_prop*, *area_chm_prop*, *area_chm_prop*, *categorical* or *ground_proportion*).**